SLAC-PUB-575

TWO-BODY PROCESSES WITH LARGE MOMENTUM TRANSFER

Martin L. Perl
Stanford University, Stanford, California, U.S.A.

1) INTRODUCTION

This review paper is concerned with the behavior of two-body processes at momentum transfers large enough to be outside the diffraction peak region. The region near 180°, where backward peaks sometimes occur in two-body processes, is also excluded. The diffraction peak region has generally been considered to extend out to about [1] $|t| = 1.0\ (\mathrm{GeV/c})^2$. Or if the second diffraction peak which occurs in some processes[2] at $|t| = 1.0$ or $1.2\ (\mathrm{GeV/c})^2$ is included in the diffraction region, then the large $|t|$ region might be started at $|t| = 1.5\ (\mathrm{GeV/c})^2$. The general concept of this region has sometimes been that the processes in this region would be hard to understand, even phenomenologically, that there would be few or no interesting effects in this region, that the nature of the particles might not be very important in this region, and that the best that could be done theoretically was to apply a statistical model.

But the large momentum transfer measurements of the last few years and the new data to be presented at this conference show many interesting and suggestive effects. There are large differences in behavior between different two-body interactions in this region. It is no longer clear that there is a theoretically

(Published in the Proceedings of Topical Conference on High-Energy Collisions of Hadrons, CERN, 15-18 January 1968. CERN 68-7-V.I:252-289)

significant separation between the small $|t|$ and the large $|t|$ parts of a two-body process. In fact, this may well be the last meeting in which such a separation is made.

This paper consists of examples and illustrations of the statements of the last paragraph. Sometimes I shall just show the data, but where I can, I shall make comparisons and try to show trends. I have usually used results with incident momenta at or above 3 (GeV/c) to avoid resonance and threshold effects. I will first discuss elastic scattering, then inelastic but true two-body interactions, and finally quasi two-body interactions.

Except for proton + proton elastic scattering there are no measurements above 12 (GeV/c) incident momentum which are relevant to this subject. Most results I will present are from the 3.0 to 7.0 (GeV/c) region. Therefore, this is perhaps more of an intermediate energy, rather than a high energy region, and we have no tests yet of truly high energy theoretical ideas.

2) <u>PROTON + PROTON ELASTIC SCATTERING</u>

Allaby et al[3] have recently made high precision measurements of p + p elastic scattering at incident momenta of 8.1 to 21.3 (GeV/c) and center-of-mass angles (θ^*) of 64° to 90°. They show their data along with the results of other experiments[4, 5, 6] in Fig. 1. The cross section $d\sigma/dt$ ($cm^2/(GeV/c)^2$)

is plotted against a special variable $s \sin\theta^*$. Here $s=4(p^{*2}+m^2)$ is the usual square of the total center-of-mass energy and m is the proton mass.

The very interesting effect is that there is a discontinuity in the data at $s \sin\theta^* \simeq 18$ GeV/c^2. This discontinuity also appears in the parameter b if at each incident momenta the data is fitted by the formula $d\sigma/dt = A \exp\left[(-p^* \sin\theta^*)/b\right]$. The paper of Allaby et al[3] should be consulted for further details.

As we proceed in this paper we will see a number of discontinuities in the various differential cross sections and I want to compare them, if possible. This requires a comment about the various parameter used to present p + p data, s, t, $s \sin\theta$ and a variable we shall use next $(\beta^* p_\perp)^2$ (Here $\beta^{*2}=(p^{*2}/p^{*2}+m^2)$ and $p_\perp = p^* \sin\theta^*$). At $\theta^* = 90^\circ$ the parameters are simply related. $s \sin\theta = s$, $(\beta^* p_\perp)^2=(s-4m^2)^2/(4s)$, $|t|=(s-4m^2)/2$. If $s \gg m^2$, $s \sin\theta = s$, $(\beta^* p_\perp)^2=s/4$ and $|t|=s/2$. Thus it is not surprizing that for θ^* near 90° say from 60 to 90°, any of these variables give reasonable plots. From the various papers, I am not clear as to which gives the best fit.

Returning to the aforementioned discontinuity, it is observed for $60^\circ < \theta^* < 90^\circ$ approximately, and I can take $\sin\theta^* \simeq .95$ and $1-\cos\theta^* \simeq .9$. Then at the discontinuity $|t| \simeq 7\,(\mathrm{GeV}/c)^2$ and $(\beta^* p_\perp)^2=2.8\,(\mathrm{GeV}/c)^2$.

Akerloff et al[4] have measured the p + p differential cross section exactly at $\theta^*=90^\circ$ from 5.0 to 13.4 GeV/c incident momentum. Their result is shown in Fig. 2 plotted versut t/2 and a discontinuity occurs at $|t|\approx 5.7(\mathrm{GeV/c})^2$. The solid line is a fit to their new data, the open and closed circles are older data. This corresponds to $(\beta^* P_\perp)^2=2.8(\mathrm{GeV/c})^2$ and is clearly the same discontinuity as seen by Allaby et al[3].

A second discontinuity in slope at small momentum transfer has been suggested by Akerloff et al[4], based on large angle data[4, 5, 6] together with small angle data[7, 8], and using $(\beta^* P_\perp)^2$ as the variable. Fig. 3, taken from Reference 4, shows a change in slope at $(\beta^* P_\perp)^2\approx 0.7(\mathrm{GeV/c})^2$. The reality of this discontinuity compared to the one at $(\beta^* P_\perp)^2=2.8(\mathrm{GeV/c})^2$ is somewhat doubtful. M. Ross[9] has pointed out that $(\beta^* P_\perp)^2=(tu)/s$ where $u= -2p^{*2}(1 + \cos\theta^*)$ in p + p elastic scattering. Then $(\beta^* P_\perp)^2=|t|(1-(4m^2+|t|)/s)$ and for $s \gg t$, $s \gg m$, $(\beta^* P_\perp)^2=|t|$. Therefore, this "break" should appear at $|t|\approx 0.7(\mathrm{GeV/c})^2$ in differential cross-section curves at high energy. But there is no evidence for this break in the individual curves.

At this conference A. N. Diddens will present very recent high prevision measurements of p + p elastic scattering at high energies. These new results show new deviations from the supposed smooth behavior of p + p elastic scattering and considerably illuminate the nature of the "break" at $(\beta^* P_\perp)^2=2.8(\mathrm{GeV/c})^2$. I refer the reader to the paper of Diddens et al in the proceedings.

A number of attempts[3, 4, 10] have been made to correct these deviations with the hadronic structure of the proton. These attempts may be premature. As we will see, other elastic scattering processes show strong deviations from smooth s and t behavior and the proper question may be -- why are the deviations in p + p elastic scattering so small? In these other processes, the deviations look like crude diffraction patterns. Can the p + p deviations be "suppressed" diffraction patterns?

In addition to the "breaks" in the curve, the other interesting thing about Fig. 3 is that the fit is independent of s to within a factor of 5 over 11 or 12 decades. This is a striking regularity, but I know of no clear explanation of this regularity.

Krisch[11] has combined all proton + proton elastic scattering data in a plot shown in Fig. 4. He plots a modified cross section $(d\sigma^+ dt)=(1/I)(d\sigma/dt)$. Where $I=1+\exp(-2a\beta^{*2}P_{\ell}^2)$ and where $P_{\ell}=P^*\cos\theta^*$. (a) has three different values depending on the $\beta^* P_{\perp}$ range. The $d\sigma^+/dt$ plot can be fitted by a sum of three exponentials in $(\beta^* P_{\perp})^2$ and is therefore independent of s. But the experimental cross section $d\sigma/dt$ depends on $\beta^* P_{\ell}$ as well as $\beta^* P_{\perp}$ and is therefore s dependent. The theoretical significance of these formulas is not clear, and as we shall show, the theory given by Krisch[11] is not correct for 90° neutron + proton elastic scattering.

Before leaving the subject of p + p elastic scattering, I wish to note that Allaby et al[6] have made a high precision search for small angular fluctuations in large angle p + p elastic scattering at 16.9 GeV/c with a null result. The possibility that "large angle elastic scattering (occurs) through random independent partial wave contributions can be excluded with a very high confidence level"[6]. The importance of this conclusion is that at least some forms of the statistical model cannot be used to explain large angle elastic scattering.

3) NEUTRON + PROTON ELASTIC SCATTERING

At this conference Cox et al[12] are presenting new data on small angle and large angle neutron + proton elastic scattering. This is additional data from the experiment of Kreisler et al[13, 14] and represents an increase by a factor of four in the statistics at large angles over that previously published[13]. I will only discuss here the cross sections for $|t| > 1.0 (\mathrm{GeV}/c)^2$ and for incident neutron momenta of 3.04 to 6.77 GeV/c. In this experiment all energies of incident neutrons were used and the data is presented for incident momentum intervals of $\pm$ .25 GeV/c (see Ref. 13).

The differential cross section data are shown in Figs. 5 and 6 for $|t|$ values greater than 1.0 $(\mathrm{GeV}/c)^2$. The $(d\sigma/dt)$ is in $[\mathrm{microbarns}/(\mathrm{GeV}/c)^2]$ and $|t|$ is in $(\mathrm{GeV}/c)^2$. The data (in the order of ascending incident momenta) is shown on alternating plots so as to get better separation. The curved lines are free-hand fits to the data. Statistical errors are shown if it is not too crowded. The vertical arrow at each curve indicates the $\theta^*=90^\circ$ point. The vertical line at the large $|t|$ end of each data set shows the maximum $|t|$ value for that incident momentum and is the $|t|$ position of the backward neutron + proton peak[15, 16, 17].

We first observe that below 4.08 GeV/c at the 90° point that $d\sigma/dt$ is still decreasing. But above 4.08 GeV/c the 90° point is just about the lowest point on the curve. Also, above 4.08 GeV/c the differential cross section is roughly symmetric about 90° for a range of $|t|$ of $\pm$ 1 or 1.5 $(\text{GeV/c})^2$. At larger $|t|$ values the curve rises toward the backward peak. But the slope at $|t|=[|t|_{90^\circ}+2](\text{GeV/c})^2$ is not as steep as the slope at $|t|=[|t|_{90^\circ}-2](\text{GeV/c})^2$. Therefore, there is not exact symmetry about 90° for $|t|$ values quite different from $|t|$ at 90°. Wu and Yang[18] have predicted just this behavior at 90°. Their idea is that it is easy for the neutron and proton to exchange their electric charge in large $|t|$ collisions. So, in fact, a neutron scattered at say $\theta^*=120^\circ$ can really be a proton scattering at 60° which has lost its charge. Also as s increases the region of symmetry about $|t|90^\circ$ should increase. From our data we cannot tell if $d\sigma/dt$ is exactly flat at 90°, but this model does not require exact symmetry.

To compare the n + p differential cross section with the p + p cross section, we first look at Fig. 7 in which the solid line gives the p + p data of Clyde[5] at 5.0 GeV/c. The circles are the n + p data at 5.10 GeV/c. It is clear that there is close agreement in the low $|t|$ region. We have not yet compared other momenta above 3.0 GeV/c because there is no suitable p + p data. At 3.0 GeV/c there is some deviation in the low $|t|$ region which we will not discuss here. Returning to Fig. 7, at $1<|t|< 2.5(\mathrm{GeV}/c)^2$ the n + p cross section may be a little lower but it is not a very strong effect. At $\theta^*=90^\circ$ the two cross sections are the same.

The 90° points can be compared at other momenta, however, and the comparison is shown in Fig. 8. The p + p data is from References 4 and 5. In this semi-logarithmic plot which is versus $|t|_{90^\circ}$ in $(\mathrm{GeV}/c)^2$ we can fit the points with the equation $(d\sigma/dt)_{90^\circ} = a \exp(-b\,|t|)$. The p + p data (solid dots) is fitted with the solid line which has the exponential slope, b = 1.64. The n + p data (open circles) falls on this line and, therefore, has the same value of b or perhaps a slightly smaller value. If we let R be the ratio of $(d\sigma/dt)_{n+p}/(d\sigma/dt)_{p+p}$, both at 90°, we find $R = 1.01 \pm .09$ averaged over the 3 to 7 GeV/c range.

There have been a number of speculations on what R might be. Krisch[11] would predict R=0.5, if we assume his "modified" cross section $d\sigma^+/dt$ (see the p + p section) is the same for p + p and n + p. Thus, the contradiction with the experiments is due to the theory being wrong or to $d\sigma^+/dt$ being different for p + p and n + p at 90°.

A general way to represent p + p and n + p scattering at 90° is as follows. Let $f_1(\theta)$ be the isotopic spin (T=1) scattering amplitude and $f_o(\theta)$ be the isotopic spin (T=0) amplitude. At 90° only symmetric space wave functions exist, therefore for T=1, S=0 and for T=0, S=1. For the p + p case $(d\sigma/dt)_{90^{\circ}}$, p + p $= |f_1(\pi/2)|^2$. For n + p the statistical weight of S=1 is 3 and of S=0 is 1, so that $(d\sigma/dt)_{90^{\circ}, n+p} = 1/4\,|f_1(\pi/2)|^2 + 3/4\,|f_o(\frac{\pi}{2})|^2$. Then for R=1.01 ± .08, $|f_o(\frac{\pi}{2})|^2 \simeq 1.0\,|f_1(\frac{\pi}{2})|^2$ or the (T=0) amplitude has a magnitude at 90° which is equal to the magnitude of the (T=1) amplitude.

Fig. 9 is a plot of the n + p data for $\theta^* > 90^{\circ}$ versus $(\beta^* P_{\perp})^2 = ut/s$. There is a crude linear behavior on this semilogarithmic plot but the point scatter is large. For incident momenta above 4.0 GeV/c the exponential slope is 2.1 $(\mathrm{GeV/c})^{-2}$. This is to be compared to the value of 3.48 $(\mathrm{GeV/c})^{-2}$ of Thus the
the exponential slope for $\theta^* < 90^{\circ}$ for p + p given in Fig. 3. This backward n + p cross-section is flatter than the forward p + p cross-section in the large angle region.

4. ANTIPROTON + PROTON ELASTIC SCATTERING

Previous to this conference there have been three published measurements of large $|t|$, $\bar{p}$ + p elastic scattering at or above 3 GeV/c. Fig. 10 shows the 3.0 GeV/c results of B. Escoubès et al[9]. The lower set of points is the $\bar{p}$ + p data and the upper set is p + p data at the same momentum. These differential cross sections are both normalized to the optical point, namely $(d\sigma/dt)/(d\sigma/dt)_o$ is plotted. This shows clearly that the $\bar{p}$ + p diffraction peak is narrower than the p + p. With this relative normalization the large $|t|$, $\bar{p}$ + p cross section is about 1/10 of the p + p cross section. But I think this relative normalization is deceptive because the large $|t|$ cross sections have no simple relation to the $(d\sigma/dt)_o$ point. Now $(d\sigma/dt)_o$, $\bar{p}$ + p is about three times $(d\sigma/dt)_o$, p + p so that in terms of absolute magnitudes the $\bar{p}$ + p, large $|t|$

cross section is about 1/3 of the p + p cross section. I will say more about this later.

Fig. 11 shows the 3.66 GeV/c results of W. M. Katz et al[20]. I have not reproduced the 40 GeV/c data of O. Czyzenski et al[21] but I shall refer to it. There is a second diffraction maximum at $|t|=.9(\text{GeV/c})^2$ clearly in the 3.66 GeV/c data and less clearly in the 3.0 GeV/c. Lower energy data at 1.5 to 2.5 GeV/c[22] show this maximum clearly so we know it exists throughout this region. As $|t|$ increases from this region into the large $|t|$ region, there is a continuous decrease of $d\sigma/dt$ through the $\theta^*=90^\circ$ point. This decrease is not completely smooth and at $|t|\approx 1.8$ (GeV/c) there is a dip and at $|t|\approx 2.0$ to 2.5 (GeV/c) there is a peak in the 3.66 GeV/c data. Higher energy data[23] to be presented at this meeting confirms the existence of these second dips and peaks. Thus, $\bar{p}$ + p, large $|t|$, elastic scattering is dramatically different from the p + p case having a richer large angle structure, a structure which apparently depends only on t. The effects we noted before for p + p were apparently more closely dependent on the variable $(\beta^* P_\perp)^2$.

Fig. 11 also shows the comparison of $\bar{p}$ + p and n + p elastic scattering at about 3.6 GeV/c. We recall that p + p is very similar to n + p so there is no need to put the p + p data on the figure. Around $|t|=1.0(\text{GeV/c})^2$ where the $\bar{p} + p$ has its second diffraction peak. The two differential cross sections are equal. Then the $\bar{p} + p$ falls rapidly but the $n + p$ drops slowly to the 90° point and falls no further. At higher momenta the same relative behavior persists. The 5.9 GeV/c data for $\bar{p} + p$ to be presented by Rubinstein et al[23] shows a rapid fall as $|t|$ increases, interrupted only slightly by the previously mentioned peak or shoulder at $|t| \approx 2.2 (\mathrm{GeV}/c)^2$.

This large $|t|$ behavior of $\bar{p} + p$ relating to $n + p$ illustrates a rough principle which we can extend to other data. In the region of incident momenta of 3.0 to 6 or 7 GeV/c and for large $|t|$ values corresponding to θ^* of a roughly 90° to 150°, the magnitude of the differential cross section is closely related to the existence of a backward scattering (180°) peak. When there are u channel processes which can give a backward peak such as in $n + p$[24], then some of these u channel processes contribute to the elastic scattering as far away as the 90° point. In that region their amplitudes mix in with the amplitudes from the small $|t|$ dominant processes. When there are no (or at least no strong) u channel processes, as in the $\bar{p} + p$ case then the large $|t|$ region depends entirely on the small $|t|$ dominant processes and the cross section decreases rapidly as $|t|$ increases. This idea is in contradiction to the statistical model idea as developed by Hagedorn[24] (see this paper for earlier references). In the Hagedorn model the 90° region is not closely related to small $|t|$ or small $|u|$ dominant processes and the differential cross section from

90° to larger angles should be roughly level. It may be that we do not yet see this behavior because we are not yet at high enough energy. When the total change in $|t|$ (or $|u|$) from 0° (180°) to 90° is only 2 to 4 $(\text{GeV}/c)^2$, as it is in the data we are discussing, we may not yet be in the statistical model region. An interesting question is how large must $\Delta|t|$ or $\Delta|u|$ be, to free the 90° region from the influence of the small $|t|$ or small $|u|$ dominant processes.

Of course, in the $\bar{p} + p$ scattering, the 90° point is of no special significance but in Fig. 8 we have plotted the $(d\sigma/dt)$ of the $\bar{p} + p$ data of References 18, 19, 21, 23. The value of b in the expression $(d\sigma/dt)90^\circ = a\exp(-b|t|)$ for $\bar{p} + p$ is 2.4 compared to 1.64 for n + p and p + p. We are then led to a very interesting speculative question. As the incident momenta increases -- will $(d\sigma/dt)90^\circ$, $\bar{p} + p$ continue to decrease faster than $(d\sigma/dt)90^\circ$, p + p or $(d\sigma/dt)90^\circ$, n + p? If this is true then for $|t| \simeq 1/2$ s (the 90° point at large s) there is no such thing as an asymptotic region. The nature of the particles will always matter.

Finally, for the $\bar{p} + p$ data I will make the following observation. Unlike $p + p_1$ and n + p we have a rather complicated structure and it is difficult to describe the cross section in a few parameters. But let me try to describe the data for $|t| > 2.0$ GeV/c by an exponential fit $(d\sigma/dt) = \alpha \exp(-\beta|t|)$ at each incident energy. We obtain:

Po=3.0 GeV/c $\alpha = 800 \pm 400\ \mu b/(GeV/c)^2$ $\beta = 1.3\ (GeV/c)^{-2}$

Po=3.66 GeV/c $\alpha = 400\ {}^{+400}_{-200}\ \mu b/(GeV/c)^2$ $\beta = 1.0\ (GeV/c)^{-2}$

Po=5.6 $\alpha = 500 \pm 300\ \mu b/(GeV/c)^2$ $\beta = 1.8\ (GeV/c)^{-2}$

Thus, compared to the diffraction peak, the exponential slope for $|t| > 2.0$ is not large. But it seems to be increasing as the $\bar{P}$ incident momentum increases. This is another way of seeing why the $(d\sigma/dt)90^{\circ}$, $\bar{p} + p$ changes more rapidly than $(d\sigma/dt)90^{\circ}$, $p + p$. There is no clear change in the value of α. These numbers are very rough. When the data of Rubenstein et al[23] is published one can make better fits, perhaps using a somewhat more complicated expression. However, there is also a great need to improve the lower energy data.

5) KAON + PROTON ELASTIC SCATTERING

The large angle differential cross section data for $K^{\pm} + p$ elastic scattering at or above 3.0 GeV/c is listed here.

System	Momentum (GeV/c)	Maximum $\|t\|$ $(GeV/c)^2$	Reference
$K^- + P$	3.0	4.3	M. N. Focacci et al[25]
$K^- + P$	3.46	2.6	J. Gordon[26]
$K^- + P$	5.9	4.6	R. Rubinstein et al[23]
$K^+ + P$	3.0	≈ 3.5	J. Debaisieux et al[27]
$K^+ + P$	3.5	5.4	W. DeBaere et al[28]
$K^+ + P$	5.0	1.5 and backward peak	W. De Baere et al[28]
$K^{\pm} + P$	3.55	Backward peak only	J. Banaigs et al[29]

Fig. 12 shows the 3.0 GeV/c K^- + P data. There is clearly a second diffraction maximum at $|t| = 1.3$ $(GeV/c)^2$ and possibly a shoulder at about 2.3 GeV/c. At 3.46 GeV/c in K^- + P, however, there is no clear evidence for either effect. I will wait for the talk of R. Rubinstein et al [23] for their conclusions as to the existence of these effects at 5.9 GeV/c in K^- + P.

In the 3.0 GeV/c K^+ + P cross section data of J. Debuisieux et al [27] there is no evidence for a second diffraction peak. There is also no evidence in the higher energy data of W. De Baere et al [28]. Of course, the statistics are not good and a dip at $|t|$=0.8 of less than 50% might be missed. K^+ + P data at 2.0 GeV/c[30] does not show a second diffraction peak either, so I am inclined to think the second peak in K^+ + P does not exist, or that it is relatively small in K^+ + P compared to K^- + P.

A good comparison and summary of $K^\pm$ + P elastic data at 3.55 GeV/c is given in Reference 29 and is presented in Fig. 13. We observe that for $|t| > 1.0$ (GeV/c) the K^+ + P and K^- + P cross sections are within a factor of two of each other, until $|t| > 4.5$ $(GeV/c)^2$. Then the backward peak in K^+ + P pulls that cross section up, whereas the K^- + P cross section continues to decrease. Statistics are clearly bad here but we can, with some optimism, see the theme I mentioned before. Backward peaks are associated with a level behavior in $(d\sigma/dt)$ at large $|t|$. If there is no backward peak $(d\sigma/dt)$ decreases continuously as $|t|$ increases. I am saying that K^+ + P is like n + p and that K^- + P is like $\bar{p}$ + p in this regard.

At roughly 3.45 to 3.66 GeV/c we can compare $\bar{p} + p$ and $K^{\pm} + P$ data using references 20, 26, 28 and 29 as shown in Fig. 14. The solid line is the $\bar{p} + p$ data if I believe the second dip at $|t|=2.0$ $(\text{GeV/c})^2$. Of course, the errors on the $\bar{p} + p$ points (which are not shown), are of the order of ±50%. We observe that for this incident momenta the large $|t|$ $\bar{p} + p$, $K^+ + P$ and $K^- + P$ differential cross sections are just about the same size out to $|t| \gtrsim 4.0$ GeV/c.

6) <u>PION + PROTON ELASTIC SCATTERING</u>

An excellent summary of $\pi^{\pm}+P$ elastic scattering from 3.0 to 6.0 GeV/c is given by C. T. Coffin et al [31]. The $(d\sigma/dt)$ behavior up to $|t|=2.5$ $(\text{GeV/c})^2$ is shown in Fig. 15 (taken from that paper). Both $\pi^+ + P$ and $\pi^- + P$ show the secondary peak at $|t| \simeq 1.2$ to 1.3 but the $\pi^- + P$ always has a larger dip at $|t| \simeq 0.8$ $(\text{GeV/c})^2$. They have no $\pi^+ + P$ data above 4.0 GeV/c at large $|t|$ but their $\pi^- + P$ data at 6.0 GeV/c shows at least a shoulder or break in the slope at $|t| \simeq 1.0$ GeV/c. Fig. 16 is a plot of the 3.0 and 4.0 $\pi^{\pm} + P$ data of Coffin et al [31]. We observe that the $\pi^- + P$ cross section is smaller than the $\pi^+ + P$ cross section large $|t|$ at the same incident momenta. Once again we see the larger backward peak (in the $\pi^+ + P$ case) associated with a higher large $|t|$ cross section. The u channel processes have a contribution out to at least $|3|(\text{GeV/c})^2$ in Δu.

Orear et al [32] have carried out $\pi^{\pm} + P$ measurements at 8 and 12 GeV/c. The $\pi^- + P$ data is shown in Fig. 17. There is clearly a shoulder at 8 and perhaps at

12 GeV/c. At first sight the 8 GeV/c $d\sigma/dt$ appears to be level at large $|t|$, but we note that for 8 GeV/c $|t|_{90} \approx 7\,(\mathrm{GeV}/c)^2$ and the data are also consistent with a decreasing cross section which I have sketched out with the heavy dotted line.

Fig. 18 shows their $\pi^+ + P$ data. A break or slope change is apparent at $|t| \approx 1\,(\mathrm{GeV}/c)^2$ at 8 and 12 GeV/c. At 8 GeV/c in the $|t| = 3$ or $4\,(\mathrm{GeV}/c)^2$ region $(d\sigma/dt)\,\pi^+ + P \approx (d\sigma/dt)\pi^- + P$. This we expect, since we are far from the backward peaks where the cross sections differ.

We now leave the $\pi^\pm + P$ data. With the new results [23] presented at this meeting there are a large number of bumps and other effects to parameterize and perhaps understand. This is clearly a task which needs doing.

I will make one comparison with other processes. Fig. 14 shows that the $\pi^+ + P$ cross section at 3.5 GeV/c and large $|t|$ (3 or 4 $(\mathrm{GeV}/c)^2$) is about the same size as the $\bar{p} + p$, $K^+ + P$ and $K^- + P$ cross sections and is about 1/10 of the p + p or n + p cross section. At 8 GeV/c and $|t| = 3\,(\mathrm{GeV}/c)^2$ the $\pi^\pm + P$ cross section is about 1/20 of the p + p cross section.

7) INELASTIC TWO-BODY INTERACTIONS

There are several inelastic, two-body interactions such as $\pi^- + P$ charge exchange, $K^- + p$ charge exchange and $\bar{p} + p \to \bar{n} + n$ for which there is no data beyond $|t|$-1.5 or 2.0 $(GeV/c)^2$. We will just note that $\pi^- + P$ charge exchange[33] shows a clear second peak at $|t| \approx 1.0$ $(GeV/c)^2$ and that $K^- + P$ charge exchange at 3.5 GeV/c does not show such a peak[34]. Other reactions such as $\bar{p} + p \to \pi^+ + \pi^-$ (Reference 35) and $\pi^- + p \to \bar{p} + d$ (Reference 36) are so rare above 3.0 GeV/c that only upper limits on the total cross section or crude total cross sections are known.

The associated production reactions

1) $\pi^- + P \to \Lambda^0 + K^0$
2) $\pi^- + P \to \Sigma^0 + K^0$
3) $\pi^- + P \to \Sigma^- + K^+$
4) $\pi^+ + P \to \Sigma^+ + K^+$

have been studied a great deal at lower energies but there is little published data above 3.0 GeV/c which can be used for our purposes. A major problem is that the cross sections are small, but a contributing problem is that many authors tend to present the angular distributions in arbitrary units and sometimes averaged over several incident momenta. Dahl et al[37] have presented an excellent summary of the three $\pi^- + P$ associated production reactions from 1.5 to 4.2 GeV/c. Fig. 19 shows the distributions. The $\Sigma^0 + K^0$ and $\Lambda^0 + K^0$

distributions have strong $\theta^*=0^o$ peaks and secondary peaks or shoulders next to this peak. (Here θ^* refers to the barycentric angle between the π^- and the K). These systems also can have small $\theta^*=180^o$ peaks at these energies and higher energies[38, 39]. The $\Sigma^- + K^+$ system has a small $\theta^*=0^o$ peak and a larger $\theta^*=180^o$ peak. We shall consider only the t region between these peaks in these systems. We define $t=(P_\pi - P_k)^2$ and $\Delta t=|t|-|t_o|$ where t_o is t at $\theta^*=0$. I have summarized the 4.0 GeV/c data below

	$(d\sigma/dt)$	$\mu b/(Gev/c)^2$	
	$\Lambda^o + K^o$	$\Sigma^o + K^o$	$\Sigma^- + K^+$
$\Delta t=1.8\ (GeV/c)^2$	0.4 ± 0.5	0.6 ± 0.8	0.0 ± 0.28
$\Delta t=3.0\ (GeV/c)^2$	0.0 ± 0.4	0.0 ± 0.8	0.2 ± 0.28
$\Delta t=4.2\ (GeV/c)^2$	0.0 ± 0.4	0.0 ± 0.8	0.6 ± 0.36
$\Delta t=5.1\ (GeV/c)^2$	0.6 ± 0.6	0.0 ± 1.2	2.0 ± 0.6

At 6.0 GeV/c Crennel et al[38] give the sum of the differential cross sections for $\pi^- + P \to \Lambda^o + K^o$ and $\pi^- + P \to \Sigma^o + K^o$. This sum is required by the difficulty of separating the two reactions at this relatively high energy and is given below

$\Delta t(GeV/c)^2$	$(d\sigma/dt)_{\Lambda^o K^o + \Sigma^o K^o}$ $\mu b/(GeV/c)^2$
3.2	$.23 \pm .09$
5.0	0
8.4	$.04 \pm .04$

In Fig. 20 I have plotted the average differential cross section $[1/2]\left[(d\sigma/dt)\Lambda^0 K^c + (d\sigma/dt)\Sigma^0 K^0\right]$ for three incident momenta 3.15, 4.0 and 6.0 GeV/c. I have also indicated the positions of the respective $\pi^- + p$ elastic differential cross sections with solid lines for 3.0 and 4.0 GeV/c data[31] and with a dashed line for 6.0 GeV/c[31, 23]. At 3.15 GeV/c the associated production cross section at $\Delta t > 2.0 (\mathrm{GeV/c})^2$ is a factor of 1/10 to 1/100 of the elastic cross section. Since the associated production cross section is fairly smooth, the variations in this factor are due to the rapidly changing elastic cross section. At 4.0 GeV/c the data is poor but for $\Delta t = 2.5 (\mathrm{GeV/c})^2$ the factor is 1/10 whereas at $\Delta t = 5 (\mathrm{GeV/c})^2$ it might be anywhere from 1/7 to 1. At 6.0 GeV/c the associated production cross section could be roughly equal to the elastic cross section at large Δt. Thus, the appearance is that as s increases the associated production large Δt cross sections decrease more slowly than the elastic cross section so that at 6.0 GeV/c they could be equal. This observation is based on very incomplete data and much better measurements are required for both associated production and elastic scattering.

The last reaction I will consider in this section is $p + p \rightarrow d + \pi^+$. This is a rather out-of-the-way reaction, but there is some data on it even at very high energies. The reaction can be studied either way, but I shall always designate the energy of the reaction by giving the incident proton kinetic energy. Heinz et al[40], Overseth et al[41] studied this reaction up to 2.8 GeV/c;

D. Dekkers et al[42] up to 4.0 GeV/c, obtaining complete angular distributions. Single $|t|$ value measurements have been made at 10.7, 14.1 GeV/c and 22.06 GeV/c by W. F. Baker et al[43], at 11.5 GeV/c by R. C. Lamb et al[44] and at 4.1 GeV/c by K. Ruddick et al[45]. The differential cross sections are, of course, symmetric about $\theta^*=90^\circ$ and show[40, 41, 42] a sharp forward peak at $\theta = 0^\circ$ at or above 2.5 GeV. Fig. 21 shows the large $|t|$ behavior in a plot of $(d\sigma/dt)/(d\sigma/dt)_{0^\circ}$ versis $P_\perp{}^2$. This normalization is not terribly important because from 2.5 to 14.1 GeV $(d\sigma/dt)_0$ decreases only from 12 μb/sr to 2.7 μb/sr. The point of the plot is that once again we see the semilogarithmic behavior versus $P_\perp{}^2$ as we did in p + p elastic scattering in Fig. 3 for the slightly different variable $(\beta^* P_\perp)^2$. There the exponential slope was 3.48 whereas in Fig. 21 it is 3.5. This exact agreement is, of course, fortuitous because we are using different parameters and the $p + p \to d + \pi^+$ cross section has been normalized. But it is very interesting that this reaction should decrease in magnitude at high energies at least roughly the same way as p + p elastic scattering.

The ratio of the $p + p \to d + \pi^+$ cross section to the p + p elastic cross section is given below

Incident proton Kinetic energy (GeV)	$\|t\|$ $(GeV/c)^2$	Ratio
4.1	3.2	4×10^{-3}
10.7	4.1	5×10^{-3}
14.1	3.4	2×10^{-3}
22.0	3.7	10^{-4}

The ratio is always very small and as the energy increases it either stays the same or decreases if the 22.0 GeV point is considered. Is this a special property of a reaction in which a deuteron is formed, or is this an indication of the very high energy behavior of other inelastic-two-body interactions?

8) INELASTIC QUASI-TWO-BODY INTERACTIONS

In this area there are many reactions and many measurements. I do not see a clear way of organizing this material and I have simply selected a few reactions to illustrate general behavior patterns. Fig. 22 shows the large $|t|$ differential cross sections[46] for the following reactions at 4.0 GeV/c

a) $\pi^+ + p \rightarrow \pi^+ + p$

b) $\pi^+ + p \rightarrow p^+ + p$

c) $\pi^+ + p \rightarrow n^{*++} + K^o$

d) $\pi^+ + p \rightarrow n^{*++} + p^o$

e) $\pi^+ + p \rightarrow n^{*++} + \omega^o$

f) $\pi^+ + p \rightarrow p + A_2^+$

All these large $|t|$ measurements (except for elastic scattering) must be regarded with some care because the question of non-resonant background subtraction is a difficult one. Note that the $d\sigma/d\Delta^2$ scale is linear here and that the $\Delta^2=|t|=0$ points are very high and are not shown. We first observe that for reactions b, d, e, and f the large $|t|$ cross section is larger than the elastic cross section in a. We also observe that the shape of $d\sigma/dt$ at large $|t|$ seems different for the different reactions, but here the question of contamination of non-resonant events may be crucial. Therefore, I have simply averaged the cross sections over the $\Delta t=2$ to $\Delta t=5$ interval, reading directly from the figure. The $\pi^+ + p$ elastic data is from Reference 31.

Products	dt range in $(GeV/c)^2$	$(d\sigma/dt)\,\mu b/(GeV/c)^2$	Ratio to elastic
$\pi + p$	2-5	4	1
$p + p$	2-5	11	2.8
$\pi^o N^{*++}$	2-5	4	1
$\rho^o N^{*++}$	2-5	8	2
$\omega^o N^{*++}$	2-4.5	14	3.5
$A_2^+ P$	2-4	19	4.7

Ratios of the differential cross sections to the elastic cross section at 4.0 GeV/c for large $|t|$ vary from 1 to 4.7. These must be taken as upper limits. But if we take these numbers as near right, we see that these quasi-two-body cross sections are the same size as the elastic cross section at large $|t|$. This is in contrast to the associated production cross sections which at this energy still are smaller than the elastic cross sections. It would be very useful to know how these cross sections vary with incident energy. However, there is no higher energy data and the large masses of the resonances make suspect the use of much lower energy data.

However, one set of reactions which have been studied[47, 48] at both large $|t|$ and high energies is $p + p \to p + n^*(1238)$, $p + p \to p + n^*(1512)$ and $p + p \to p + n^*(1688)$. I have listed below the 7.1 GeV/c data of Ankenbrandt et al[47]. The ratio is that of the $(d\sigma/dt)$ for the resonance to the elastic $(d\sigma/dt)$ at the same $|t|$ value. The ratios given by Ankenbrandt et al[47] are to the elastic $(d\sigma/dt)$ at $|t|=5.44(GeV/c)^2$.

N^* Mass	$\|t\|$ $(GeV/c)^2$	$(d\sigma/dt)_{m^*+p}$ $\frac{\mu b}{(GeV/c)^2}$	Ratio
1238	5.06	.12 ± .12	.15 ± .15
1520	4.59	1.5 ± .75	1.5 ± .75
1690	4.24	.78 ± .39	.62 ± .31

Fig. 23 shows the higher energy data of E. W. Anderson et al[48]. We see that for large $|t|$ the $(d\sigma/dt)$ for the $N^*(1520)$ or $N^*(1690)$ is about 1/3 of the $(d\sigma/dt)$ elastic at the same $|t|$ and s value. This is in contrast to the 7.1 GeV/c data where the cross sections are of the same size. If we accept all the data as presented, then for large $|t|$ the ratio of $(d\sigma/dt)_{N^* + p}$ to $(d\sigma/dt)_{p + p}$ elastic seems to decrease as s increases, at least for a while. Here again, we need more information. Finally, we note that at fixed s the exponential slope of the $(d\sigma/dt)_{N^* + p}$ is about 1.5 $(GeV/c)^{-2}$.

Thus, there appears to be a difference in behavior between the behavior of a true two-body inelastic process like associated production and a quasi-two-body inelastic process like $p + p \to N^* + p$. The associated production, large $|t|$ cross section is much less than the $\pi^- + p$ elastic cross section at low s but is equal to it at higher s. The $p + p \to N^* + p$, large $|t|$, cross section is equal to the p + p elastic cross section at low s but becomes smaller at high s. This observation cannot be pressed too hard at present because the data is so sketchy, but we can make a strong negative statement: There is no experimental proof for the general statement that as s increases the largest differential cross sections of elastic, true-two-body inelastic and quasi-two-body inelastic will become roughly equal.

For a final example, we consider the reaction $K^+ + p \rightarrow K^{*o}(890) + N^{*++}(1238)$ with $K^{*o}(890) \rightarrow K^+ + \pi^-$ and $N^{*++}(1238) \rightarrow p + \pi^+$. Using references 49 and 50, we have compiled the following comparison. $d\sigma/dt$ is the differential cross section for the reaction in $\mu b/(GeV/c)^2$. R is the ratio of that cross section to the $K^+ + p$ elastic cross section[27, 28] at the same s and t values

Incident Momentum (GeV/c)	Δt $(GeV/c)^2$ 1.5		2.5		3.5	
	$d\sigma/dt$	R	$d\sigma/dt$	R	$d\sigma/dt$	R
3.0	90	$1.2 \pm .5$	40	2.2 ± 1.2		
3.5	80	$1.3 \pm .5$	20	$.9 \pm .5$	3	$.4^{+.6}_{-.2}$
5.0	80		10		13(?)	

With the large errors, all we can say is that this quasi-two-body interaction has about the same cross section as the elastic scattering in the 3 to 3.5 GeV/c momentum interval. With respect to the increase of momentum, the $\Delta t = 1.5 (GeV/c)^2$ cross section seems independent of the incident momentum, but the $\Delta t = 2.5\ (GeV/c)^2$ cross section decreases. At a fixed momentum of 3.5 GeV/c, the exponential slope is ~ 1.8 $(GeV/c)^{-2}$ with respect to Δt.

With these remarks the survey is ended. There is clearly much theoretical work and much more experimental work needed in this region. With respect to theoretical thought, we do not even know how to parameterize this region. With respect to experimental work in many cases the data are scattered, the errors are large and the contamination is uncertain. Even for simple elastic scattering more measurements are needed for almost all systems at 4.0 GeV/c and above. Only the p + p elastic scattering data are in reasonable shape, although they are not as complete as they might be.

References

1. In this paper, the four-momentum transfer squared t is defined by $t=(p_2 - p_1)^2$ where p_1 is the four-momentum of the incident particle and p_2 is the four-momentum of one the produced particles. We use $p^2=m^2$ where m is the particle mass. In elastic scattering, p_2 is taken to be the same particle as the incident particle. In inelastic two-body processes, the particle to which p_2 is assigned will be specified. t is always negative in elastic scattering.

2. See, for example, C. T. Coffin et al, Phys. Rev. 159, 1196 (1967).

3. J. V. Allaby et al, Phys. Letters 25B, 156 (1967).

4. C. W. Akerloff et al, Phys. Rev. 159, 1138 (1967).

5. A. R. Clyde, Ph.D. Thesis, U.C.R.L. 16275 (unpublished).

6. J. V. Allaby et al, Phys. Letters 23, 389 (1966).

7. K. J. Foley et al, Phys. Rev. Letters 10, 376, 543 (1963); 11, 425, 503 (1963); 14, 862 (1965); 15, 45 (1965).

8. G. Cocconi et al, Phys. Rev. Letters 11, 499 (1963); 12, 132 (1964): Phys. Rev. 138, B165 (1965).

9. M. Ross, Univ. of Mich., private communication.

10. M. M. Islam and J. Rosen, Phys. Rev. Letters 19, 178 (1967)(and Errata, Phys. Rev. Letters 19, 1360 (1967)).

11. A. D. Krisch, Phys. Rev. Letters 19, 1148 (1967).

12. J. Cox, M. L. Perl, M. Longo, M. Kreisler (unpublished data presented at this conference).

13. M. N. Kreisler et al, Phys. Rev. Letters 16, 1217 (1966).

14. M. N. Kreisler, Ph.D. Thesis, SLAC Report No. 66.

15. H. Palevsky et al, Phys. Rev. Letters 9, 509 (1962).
J. L. Friedes et al, Phys. Rev. Letters 15, 38 (1965).

16. G. Manning et al, Nuovo Cimento 41A, 167 (1966).

17. M. J. Longo et al, (unpublished data presented at this conference).

18. T. T. Wu and C. N. Yang, Phys. Rev. 137, B708 (1965).

19. B. Escoubès et al, Phys. Letters 5, 132 (1963).

20. W. M. Katz et al, Phys. Rev. Letters 19, 265 (1967).

21. O. Czyzewski et al, Phys. Letters 15, 188 (1965).

22. B. Barish et al, Phys. Rev. Letters 17, 720 (1966).

23. R. Rubinstein et al, (unpublished data presented at this conference).

24. R. Hajedorn Nuovo Cimento 35, 216 (1965).

25. M. N. Focacci et al, Phys. Letters 19, 441 (1965).

26. J. Gordon, Phys. Letters 21, 117 (1960).

27. J. Debaisieux et al, Nuovo Cimento 43A, 143 (1966).

28. W. DeBaere et al, Nuovo Cimento 45A, 885 (1960).

29. J. Banaigs et al, Phys. Letters, 24B, 317 (1967).

30. W. Chinowsky et al, Phys. Rev., 139 B1411 (1965).

31. C. T. Coffin et al, Phys. Rev. 159, 1169 (1967).

32. J. Orear et al, Phys. Rev. 152, 1162 (1966).

33. P. Sonderegger et al, Phys. Letters, 20, 75 (1966).

34. A. D. Brody and L. Lyons, Nuovo Cimento

35. T. Ferbel et al, Phys. Rev. 143, 1096 (1966).

36. M. Perl et al, Phys. Rev. 132, 1273 (1963).

37. O. I. Dahl et al, Phys. Rev. 163, 1430 (1967).

38. D. J. Crennell et al, Phys. Rev. Letters, 18, 86 (1967).

39. T. F. Hoang et al, Phys. Letters 25B, 615 (1967).

40. R. M. Heinz et al, University of Michigan Report (1967) (unpublished).

41. O. E. Overseth et al, Phys. Rev. Letters 13, 59 (1964).

42. D. Dekkers et al, Phys. Letters 11, 161 (1964).

43. W. F. Baker et al, Phys. Rev. 136, B779 (1963).

44. R. C. Lamb et al, Phys. Rev. Letters 17, 100 (1966).

45. K. Ruddick et al, (to be published).

46. Aachen-Berlin-Birmingham-Bonn-Hamburg-London-Munchen Collaboration, Phys. Rev. 138B, 897 (1965).

47. C. M. Ankenbrandt et al, Nuovo Cimento 35, 1053 (1965).

48. E. W. Anderson et al, Phys. Rev. Letters 16, 855 (1966).

49. M. Ferro-Luzzi et al, Nuovo Cimento 39, 432 (1965).

50. R. George, Nuovo Cimento 49, 9 (1967).

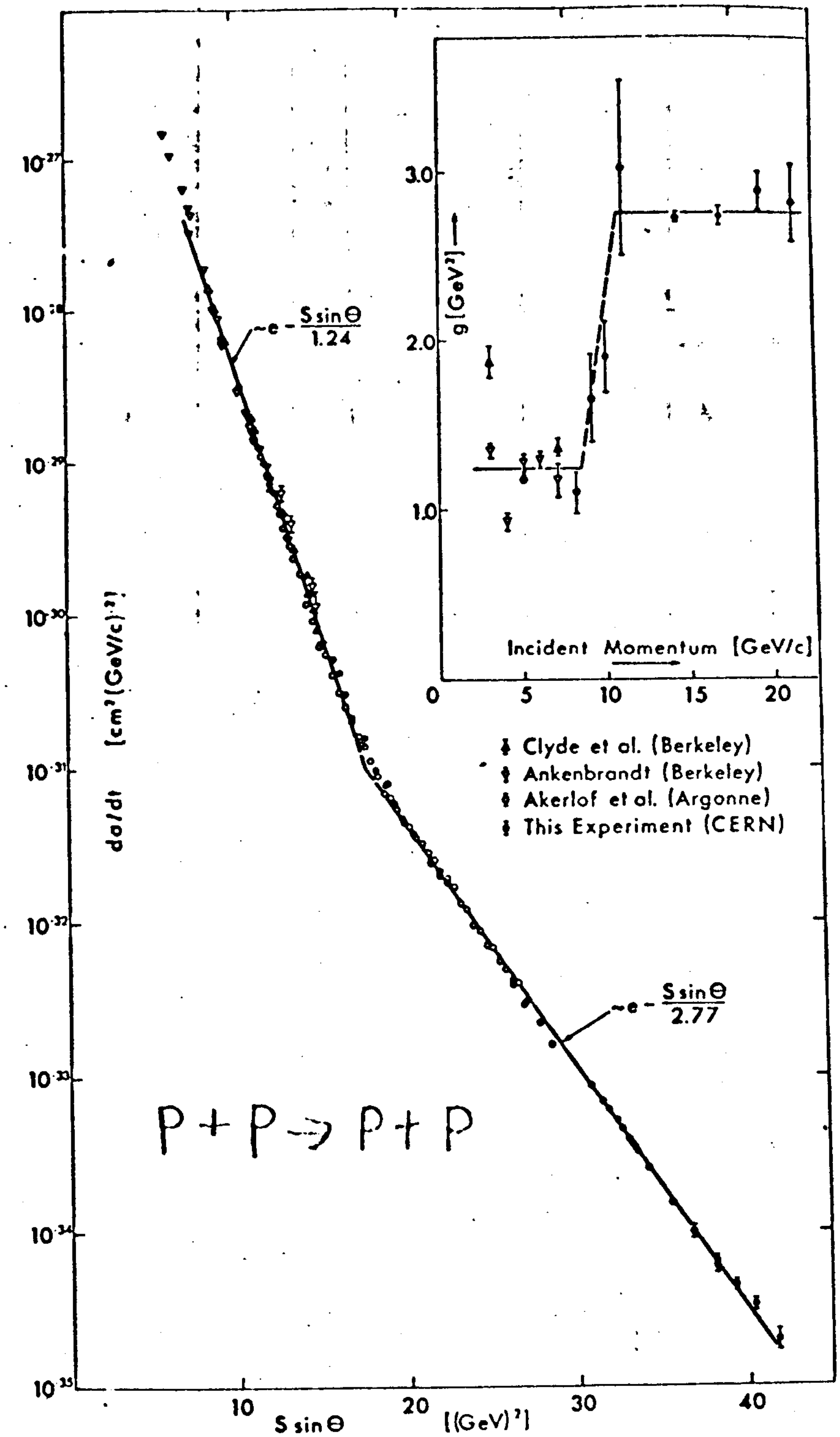

Fig 1 Logarithmic plot of $(d\sigma/dt)$ as a function of $s \sin\Theta$. The data are from Clyde et al. [3], Ankenbrandt [7], Akerlof et al. [8] and the present experiments. The lines in the figure result from a fit to the points by $(d\sigma/d\ ) \propto \exp(-s \sin \Theta/g)$. The inset gives values of g obtained from the individual angular distributions, the two horizontal lines indicating the values obtained from the overall fit shown in the figure.

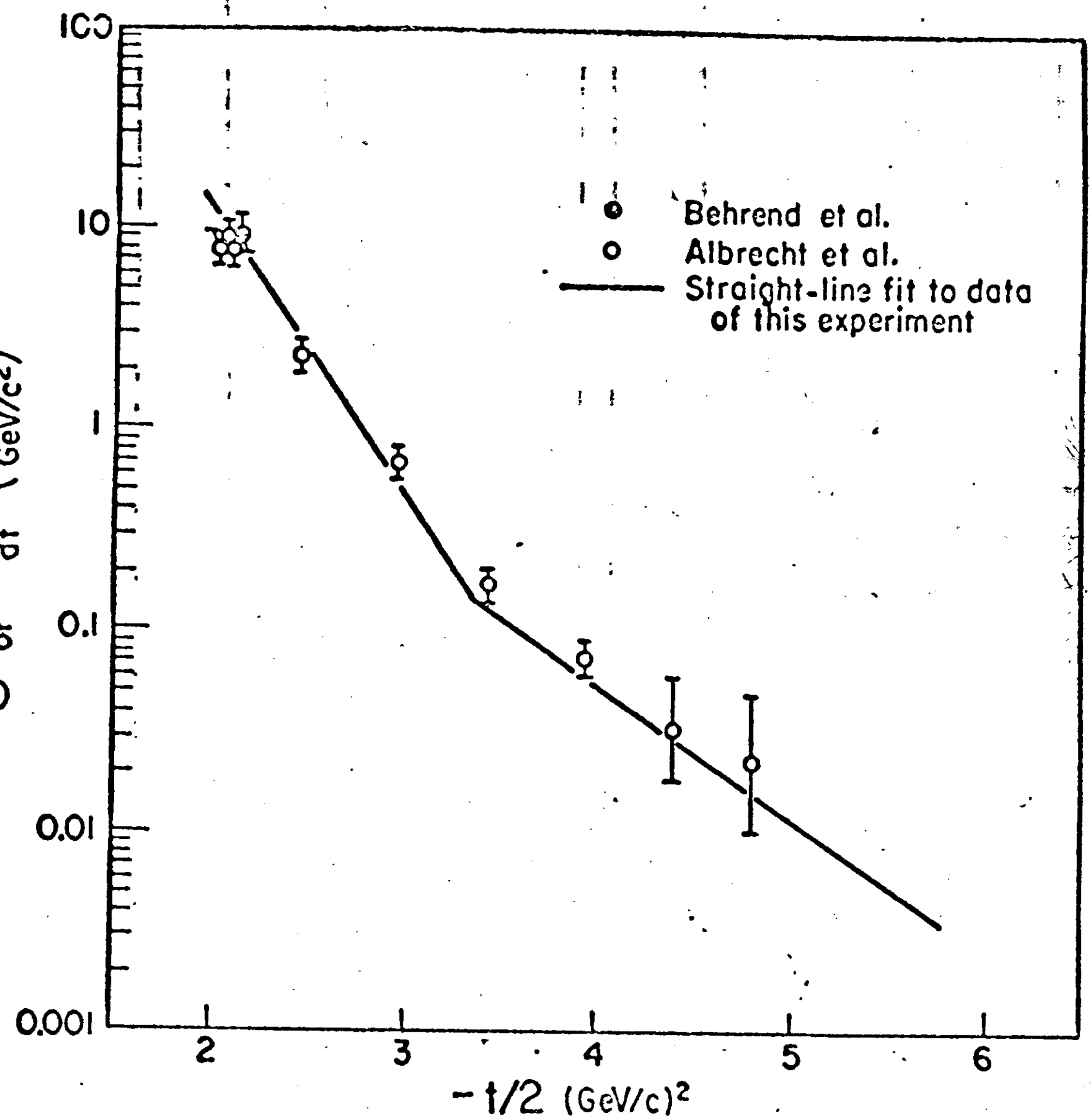
100
10
1
0.1
0.01
0.001
G^4 or $\frac{d\sigma}{dt}$ $\left(\frac{\mu b}{GeV/c^2}\right)$
2
3
4
5
6
$-t/2$ $(GeV/c)^2$
Behrend et al.
Albrecht et al.
Straight-line fit to data of this experiment

Fig. 2

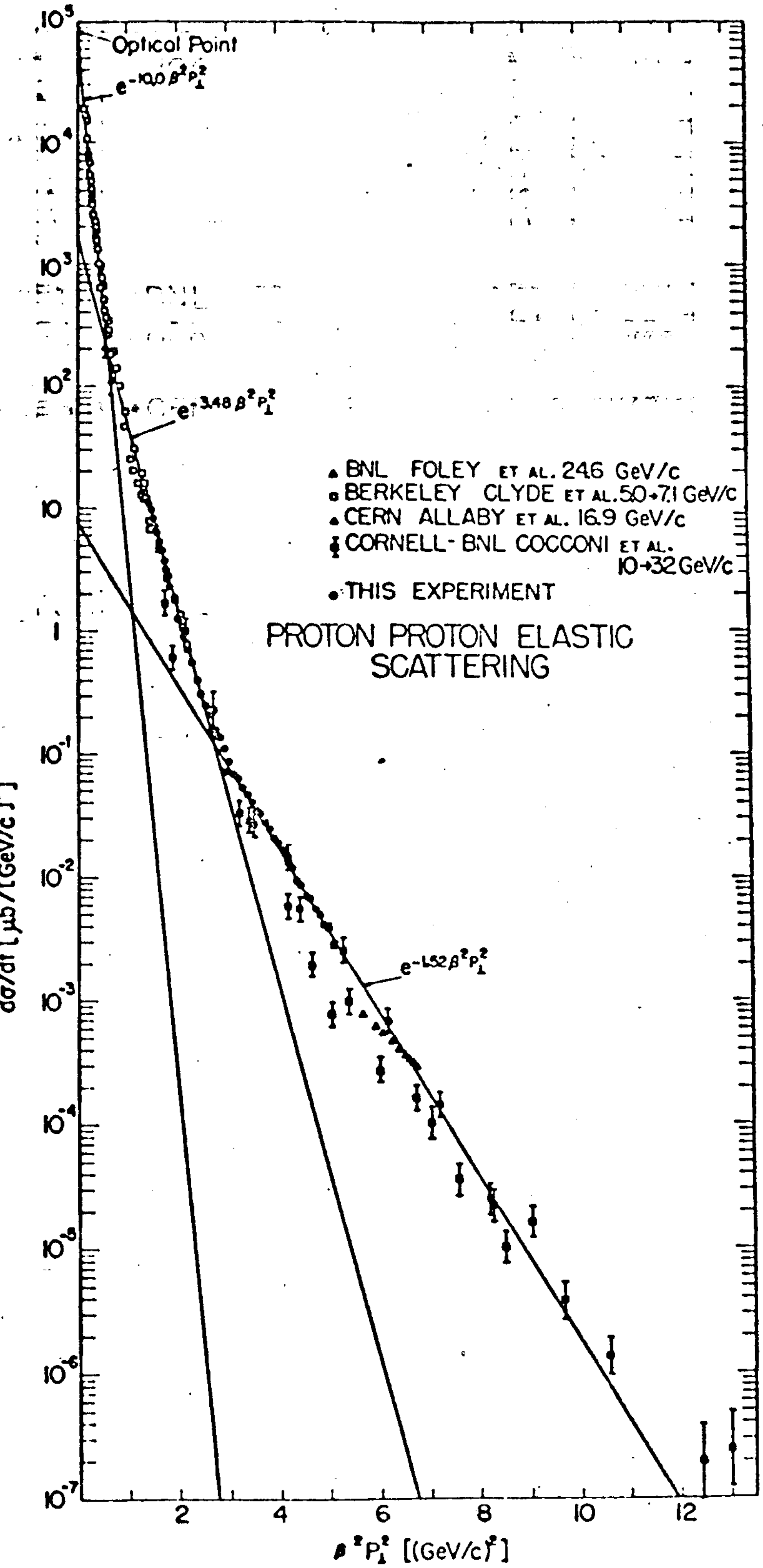
Optical Point
$e^{-10.0\beta^2 P_\perp^2}$
$e^{-3.48\beta^2 P_\perp^2}$
$e^{-1.52\beta^2 P_\perp^2}$
BNL FOLEY ET AL. 24.6 GeV/c
BERKELEY CLYDE ET AL. 5.0→7.1 GeV/c
CERN ALLABY ET AL. 16.9 GeV/c
CORNELL-BNL COCCONI ET AL. 10→32 GeV/c
THIS EXPERIMENT
PROTON PROTON ELASTIC SCATTERING
dσ/dt [μb/[GeV/c]²]
$\beta^2 P_\perp^2$ [(GeV/c)²]

Fig. 3

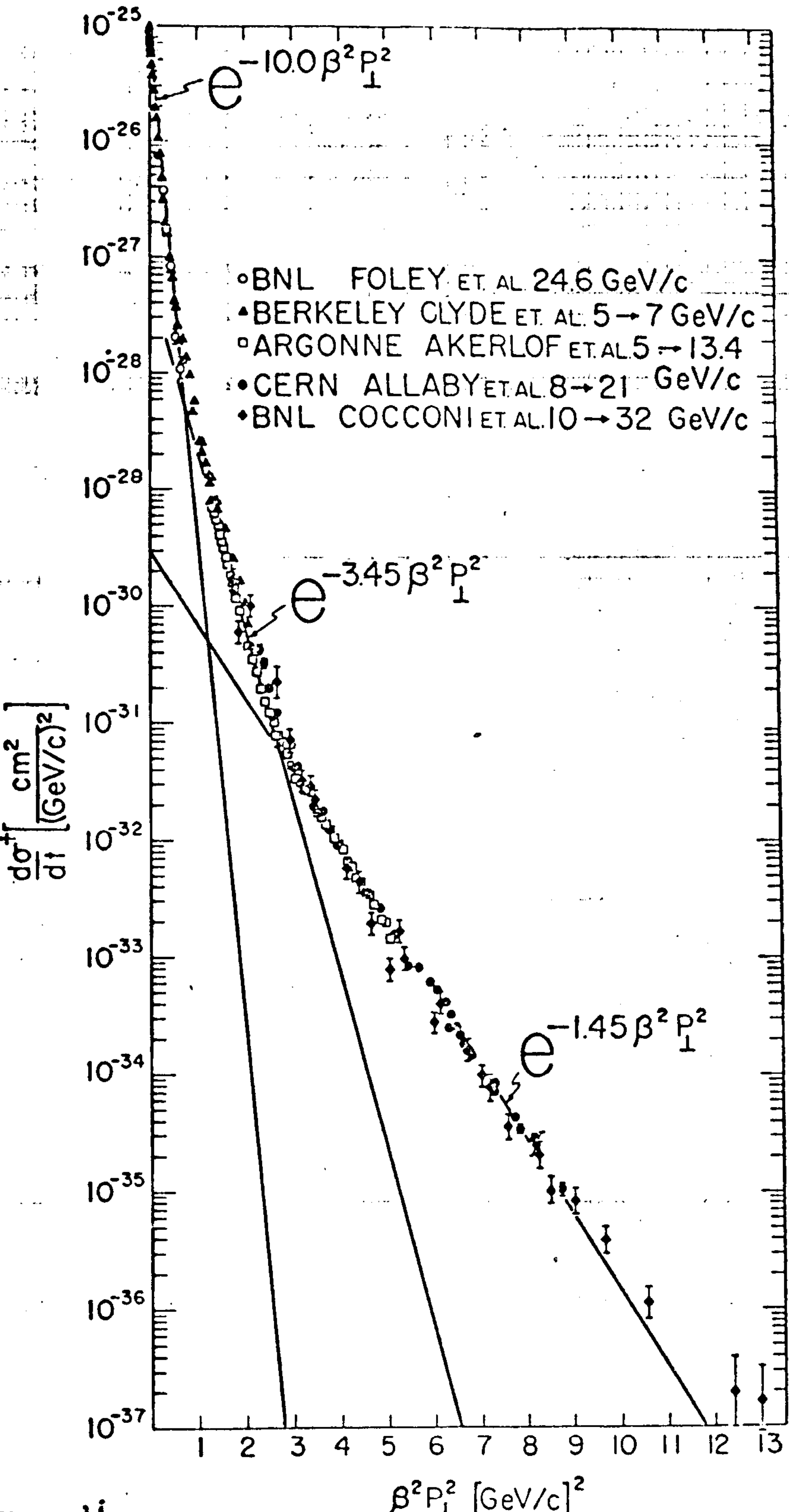

Fig 4 Plot of $d\sigma^\dagger/dt$ vs $\beta^2 P_\perp{}^2$ for all high-energy proton-proton elastic-scattering data . Not all small-angle data (are snown on this plot to avoid crowding.

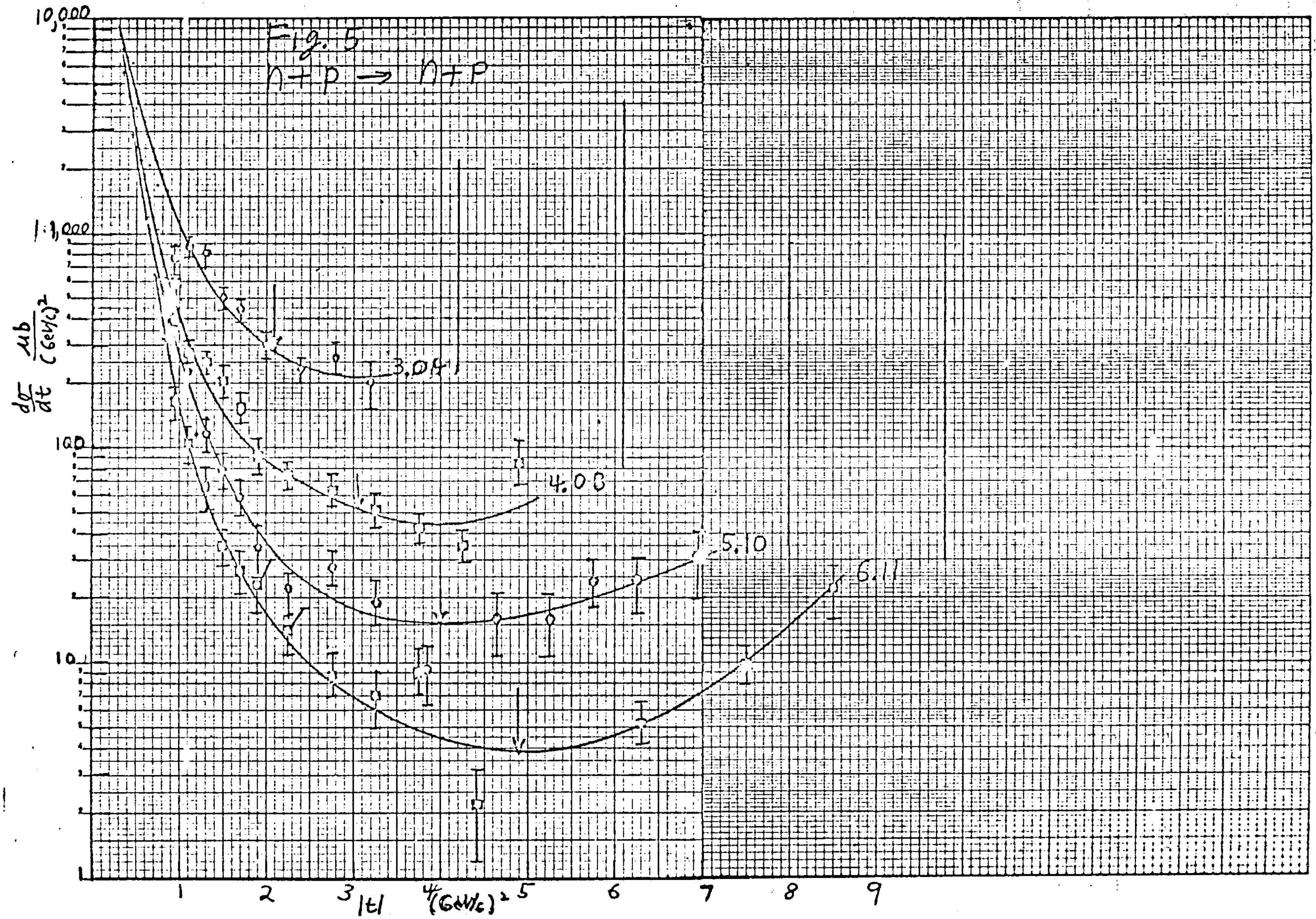

Fig. 5
n + p → n + p
10,000
1,000
100
10
1
$\frac{d\sigma}{dt}$ $\frac{\mu b}{(GeV/c)^2}$
3.04
4.08
5.10
6.11
1
2
3
4
5
6
7
8
9
|t| $(GeV/c)^2$

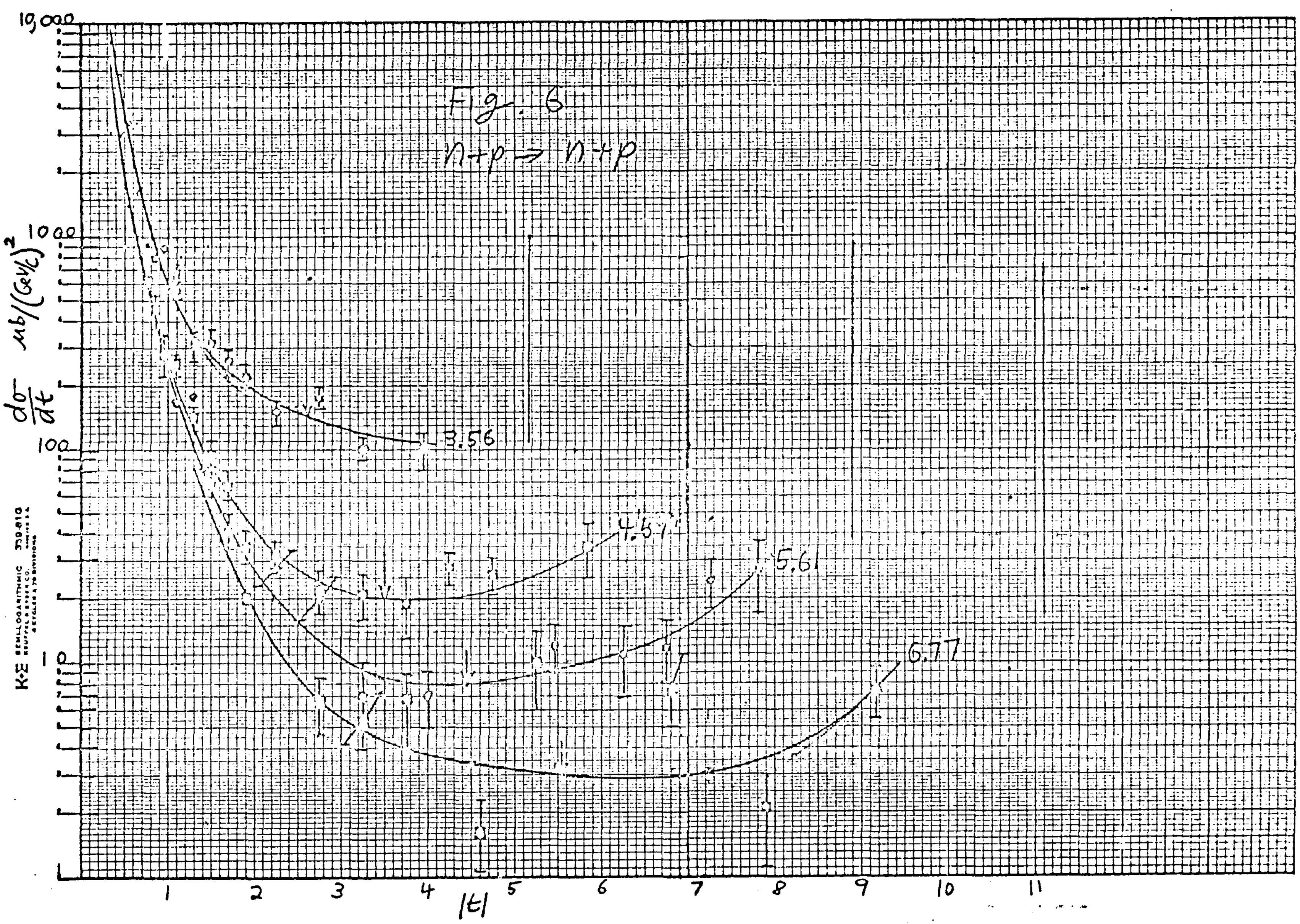

Fig. 6
n+p → n+p
10,000
1000
100
10
1
$\frac{d\sigma}{dt}$ $\mu b/(GeV/c)^2$
3.56
4.57
5.61
6.77
1
2
3
4
5
6
7
8
9
10
11
|t|

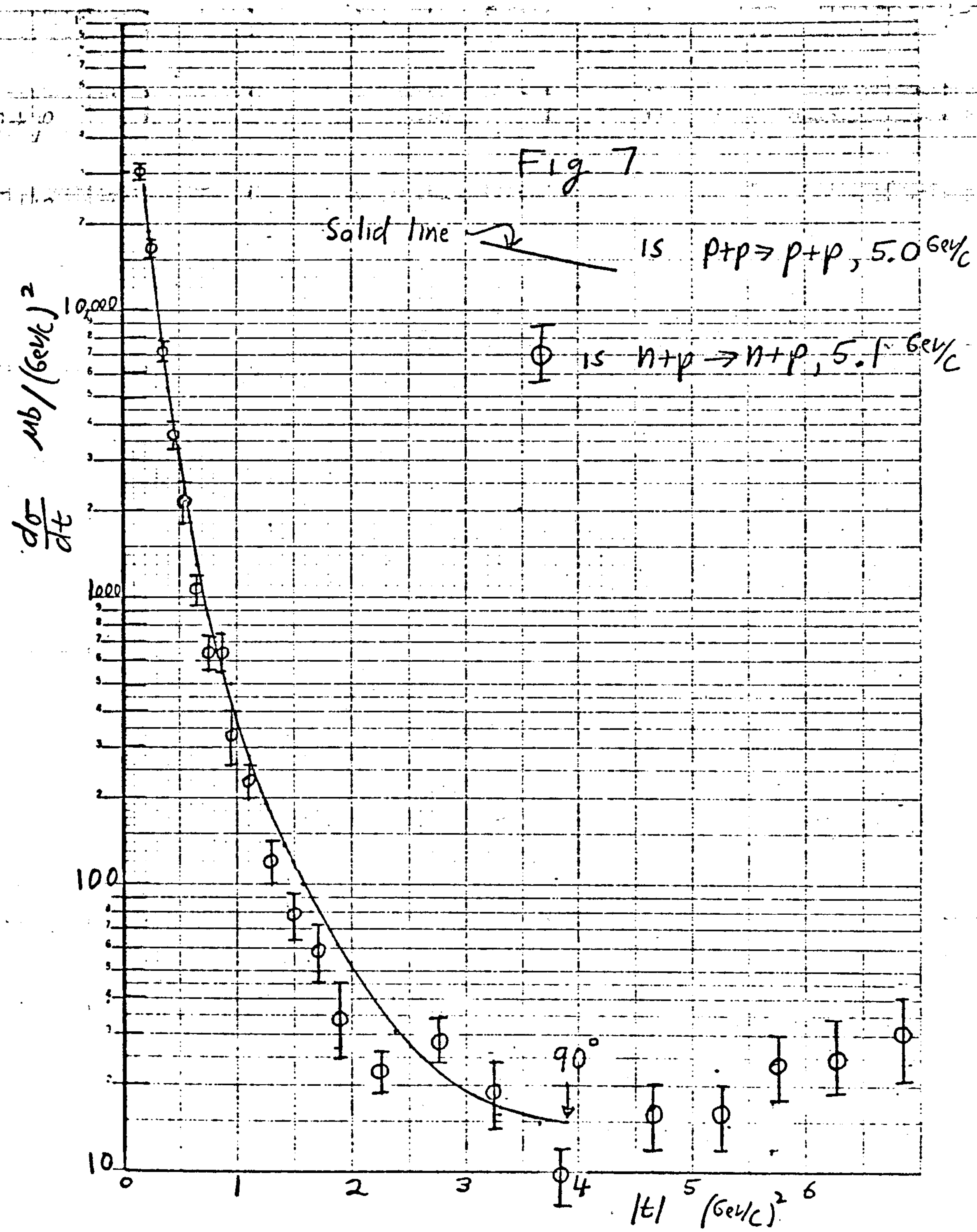

Fig 7
Solid line is p+p → p+p, 5.0 GeV/c
is n+p → n+p, 5.1 GeV/c
dσ/dt μb/(GeV/c)^2
10,000
1000
100
10
90°
0
1
2
3
4
5
6
|t| (GeV/c)^2

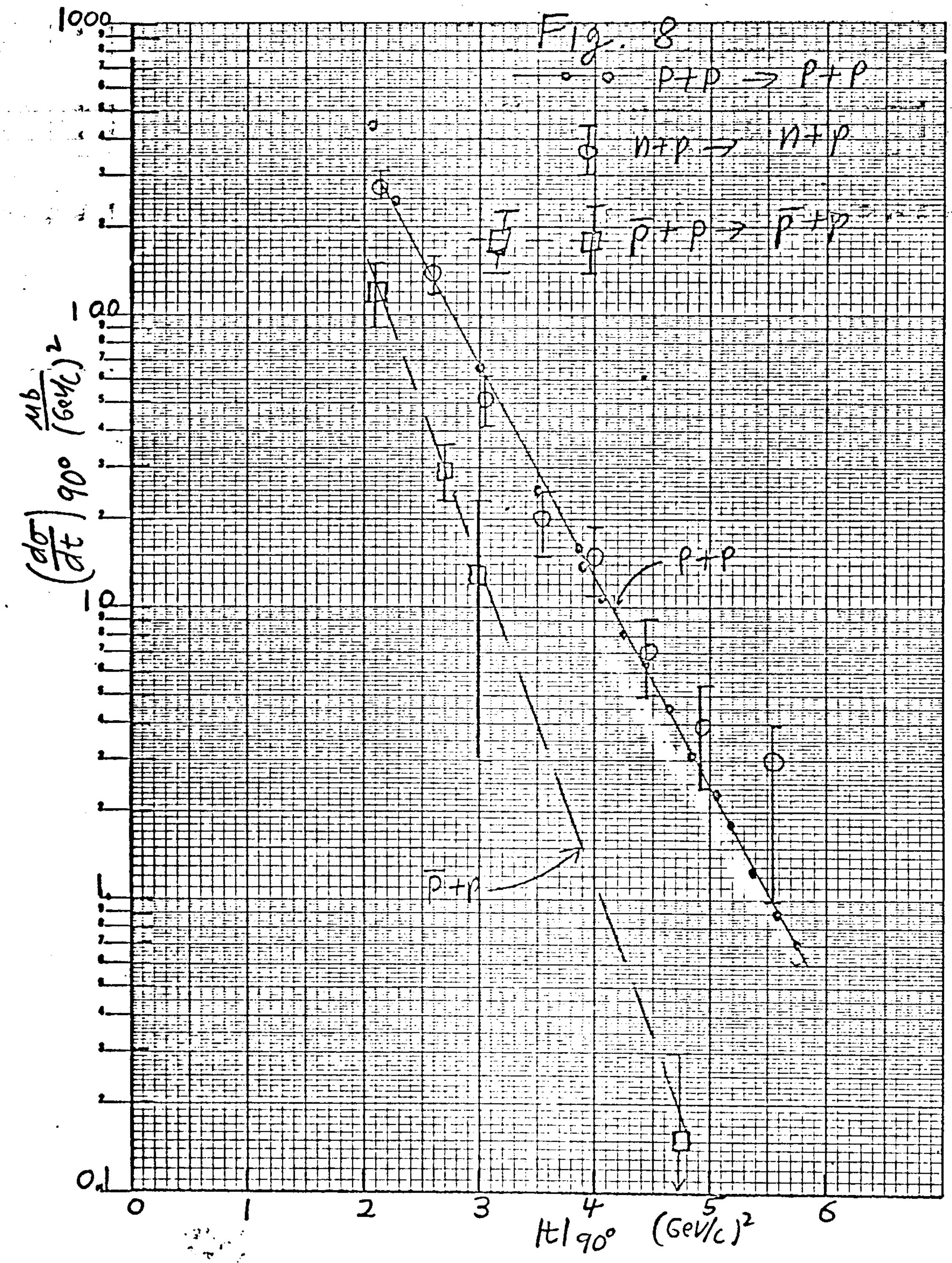
Fig. 8
p+p → p+p
n+p → n+p
p̄+p → p̄+p
p+p
p̄+p
1000
100
10
1
0.1
0
1
2
3
4
5
6
(dσ/dt)90° mb/(GeV/c)²
|t|90° (GeV/c)²

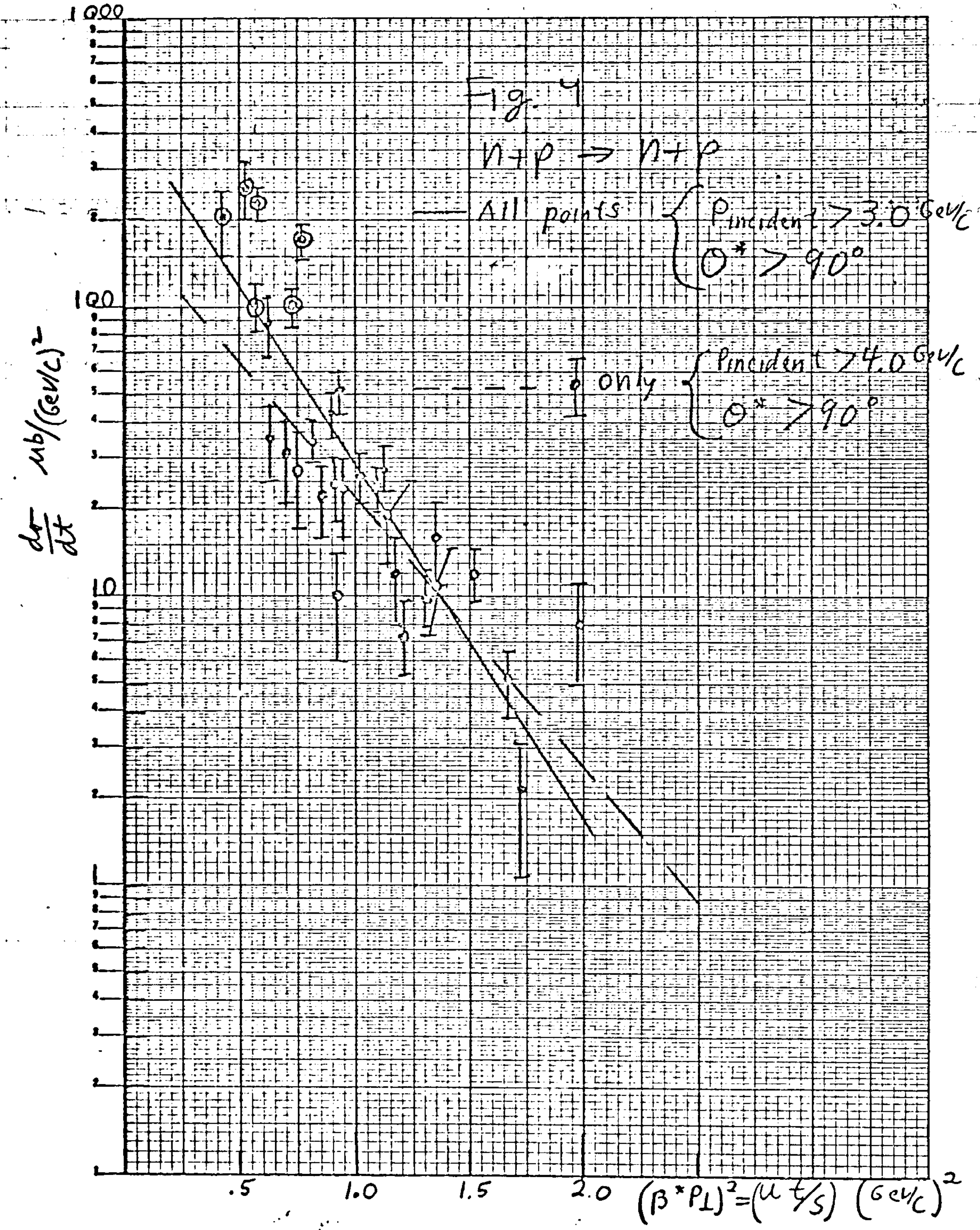

Fig. 4
n+p → n+p
All points { P incident > 3.0 GeV/c, θ* > 90°
only { P incident > 4.0 GeV/c, θ* > 90°
1000
100
10
1
.5
1.0
1.5
2.0
(β* P⊥)² = (u t/s) (GeV/c)²
dσ/dt μb/(GeV/c)²

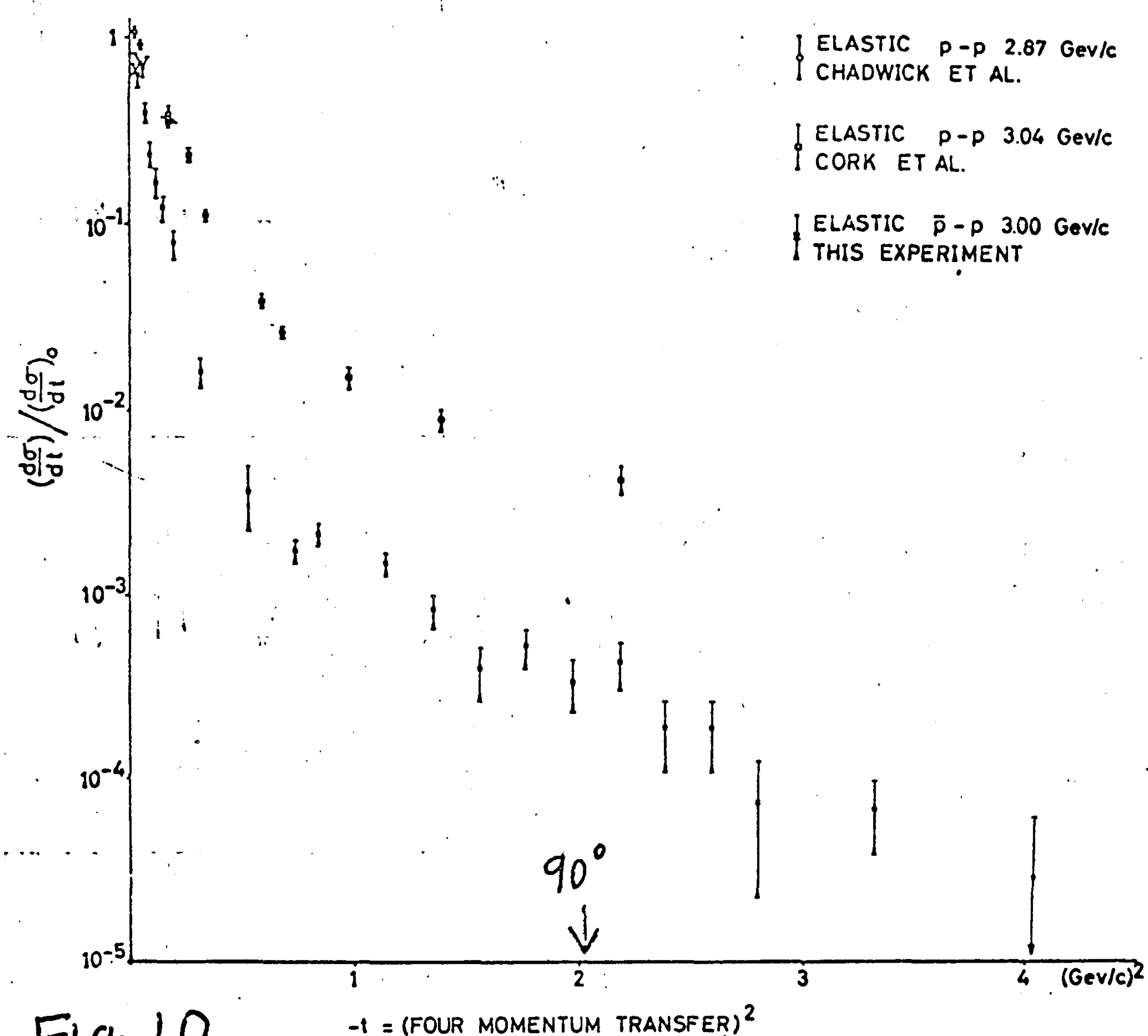

Fig. 10. Elastic pp and p̄p differential cross sections normalised to corresponding optical theorem points.

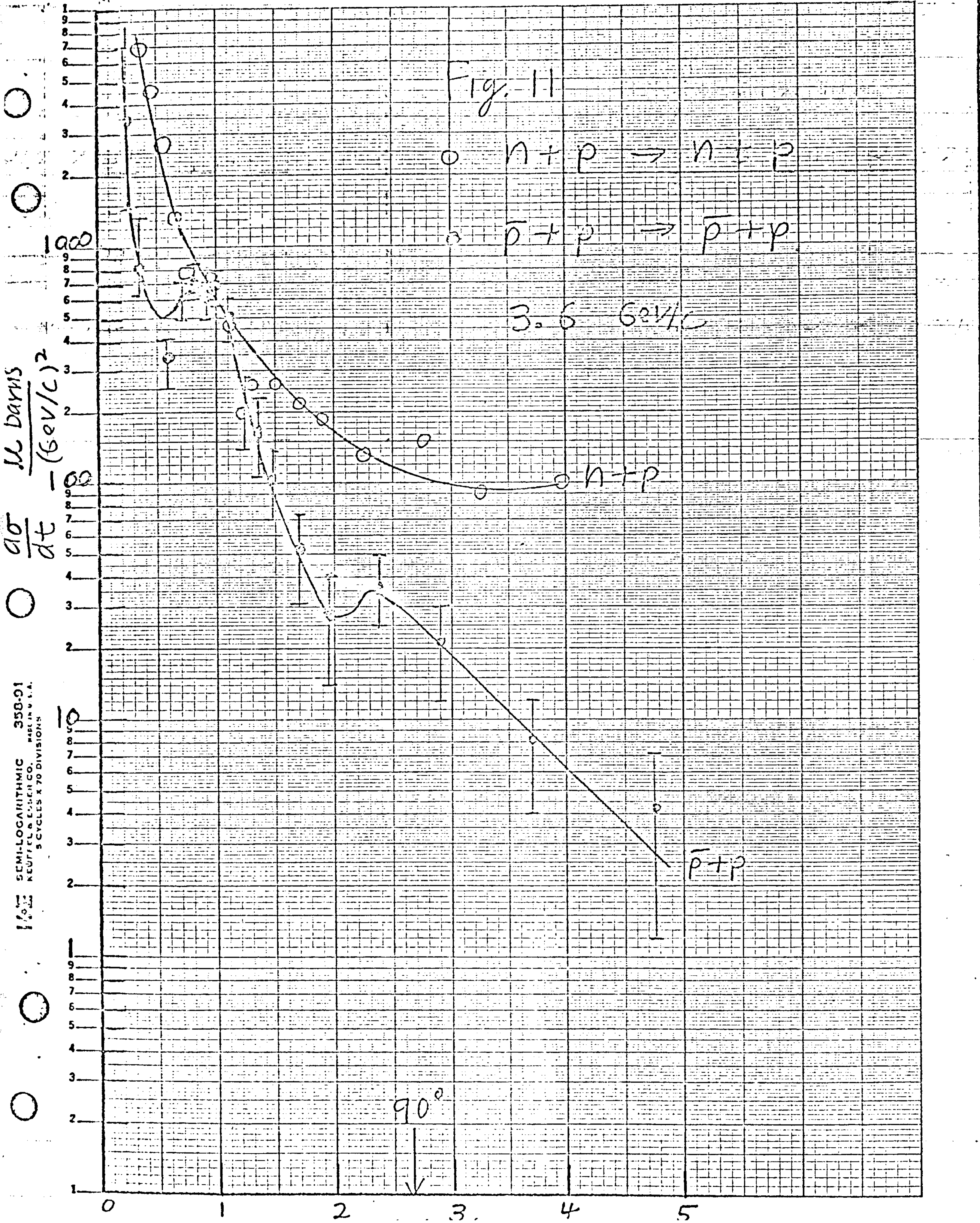

Fig. 11
n + p → n + p
p̄ + p → p̄ + p
3.6 GeV/c
n+p
p̄+p
$\frac{d\sigma}{dt}$ $\frac{\mu\ barns}{(GeV/c)^2}$
1000
100
10
90°
0
1
2
3
4
5
SEMI-LOGARITHMIC 358-91
KEUFFEL & ESSER CO. MADE IN U.S.A.
5 CYCLES X 70 DIVISIONS

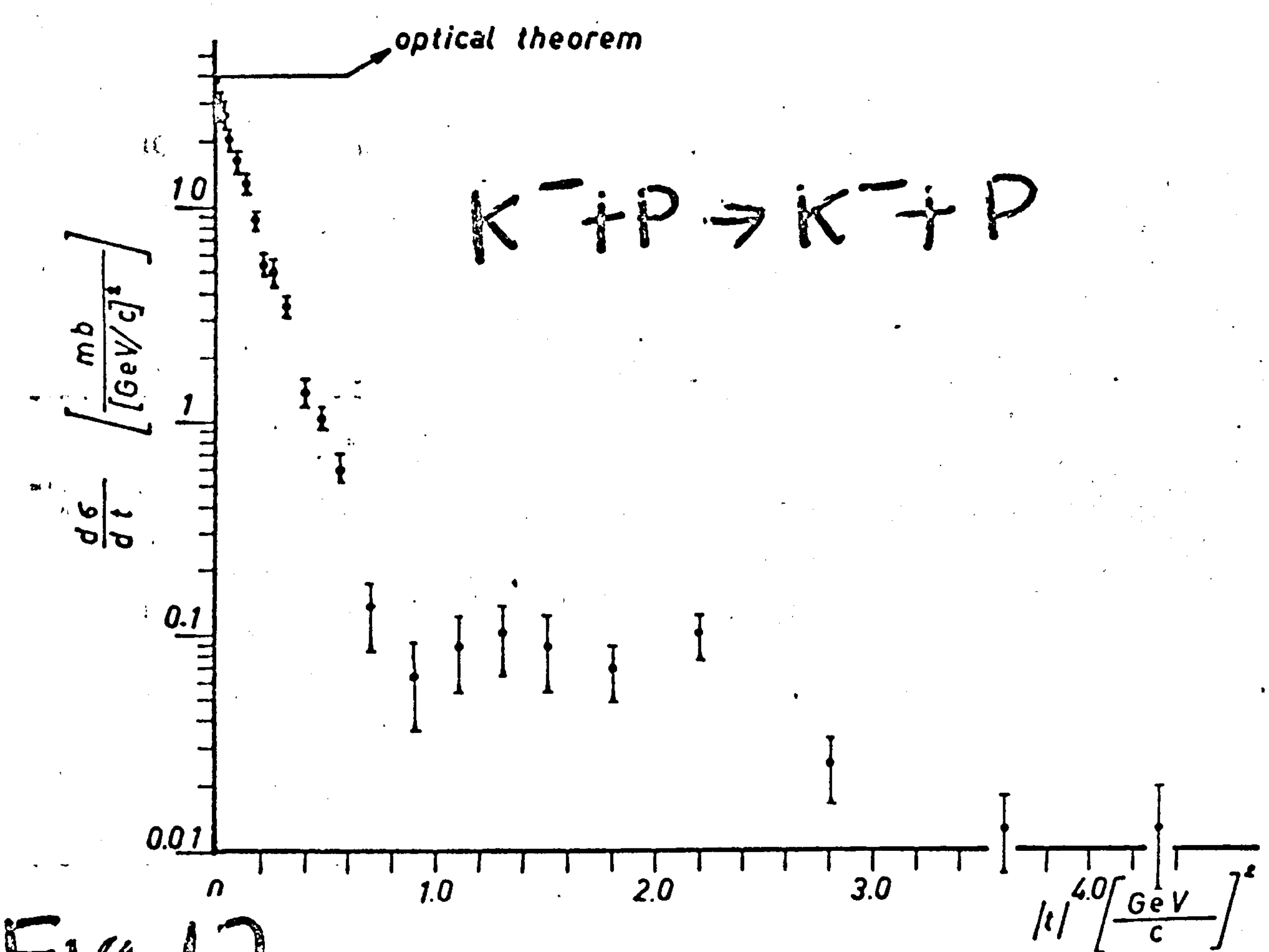

Fig. 12 Measured differential elastic scattering cross sections expressed as $d\sigma/dt$ versus $|t|$. The errors shown are standard deviations and include statistical uncertainties only.

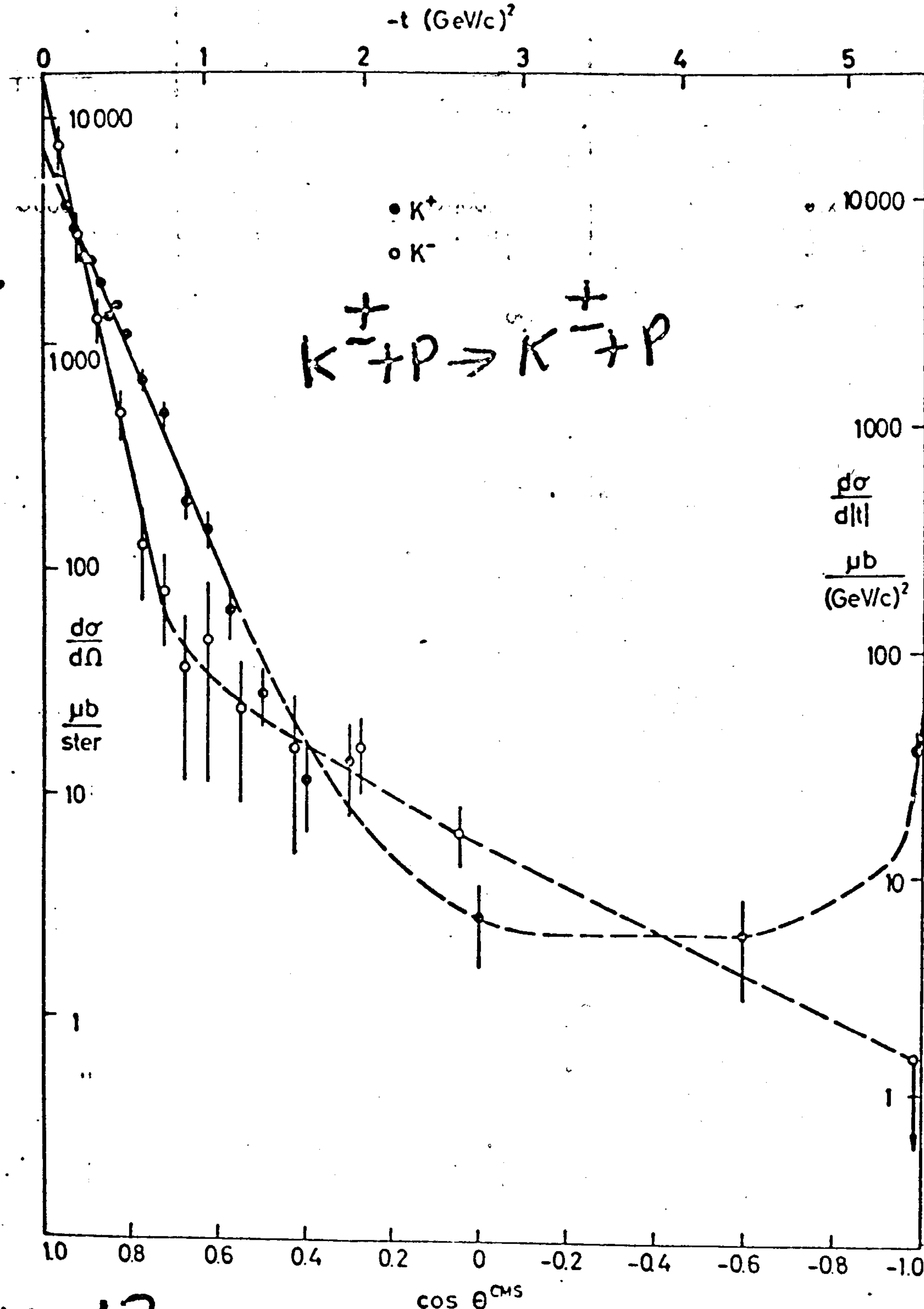

Fig. 13. The angular distributions of $K^{\pm}p$ elastic scattering. The non-backward parts are from refs. 2 and 3, taken at 3.5 GeV/c. The dotted curves indicate the gross features of the angular distributions.

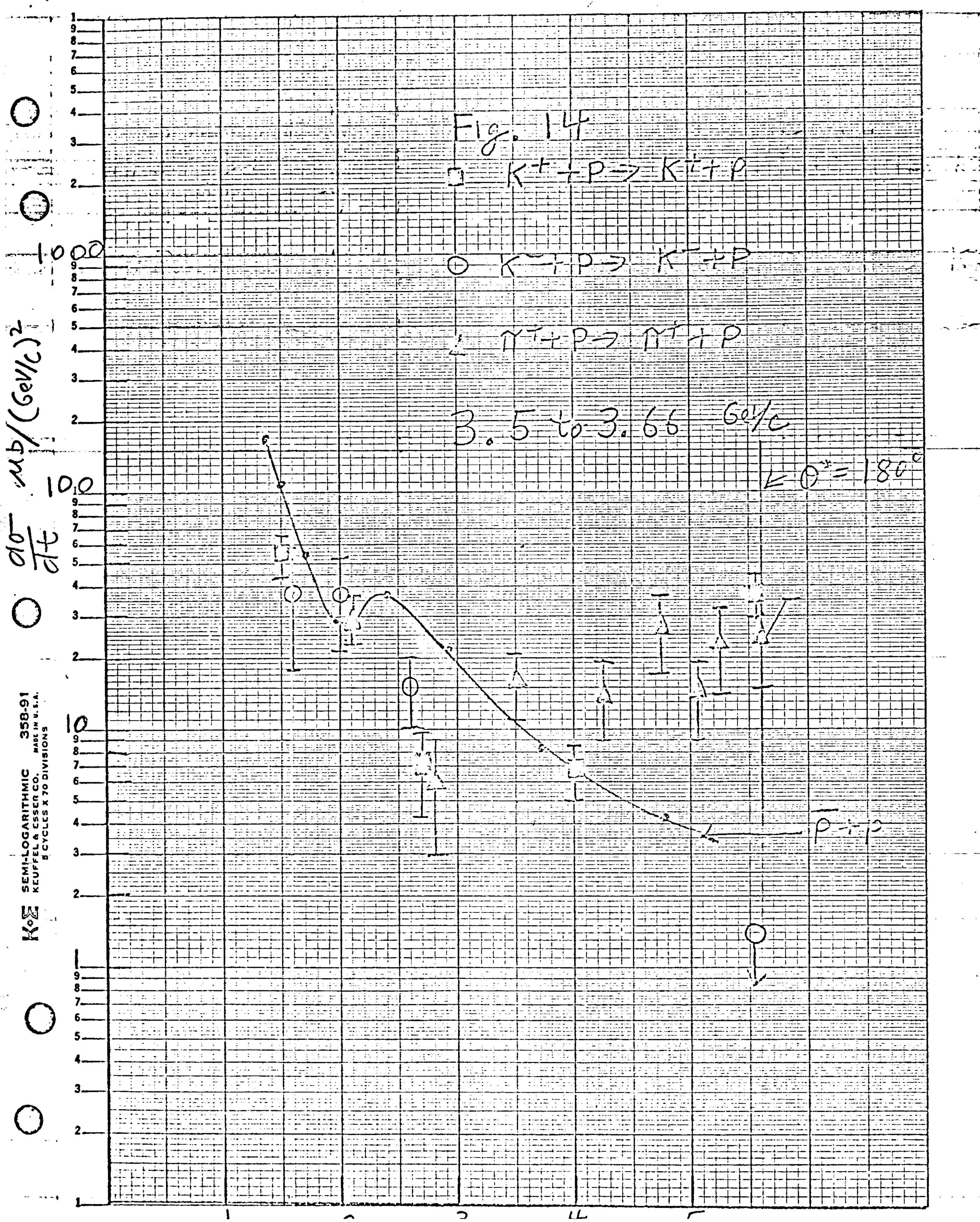
Fig. 14
□ K⁺ + P → K⁺ + P
○ K⁻ + P → K⁻ + P
△ π⁺ + P → π⁺ + P
3.5 to 3.66 GeV/c
∠θ* = 180°
P + P
dσ/dt μb/(GeV/c)²
1000
100
10
SEMI-LOGARITHMIC 358-91
KEUFFEL & ESSER CO. MADE IN U.S.A.
5 CYCLES X 70 DIVISIONS

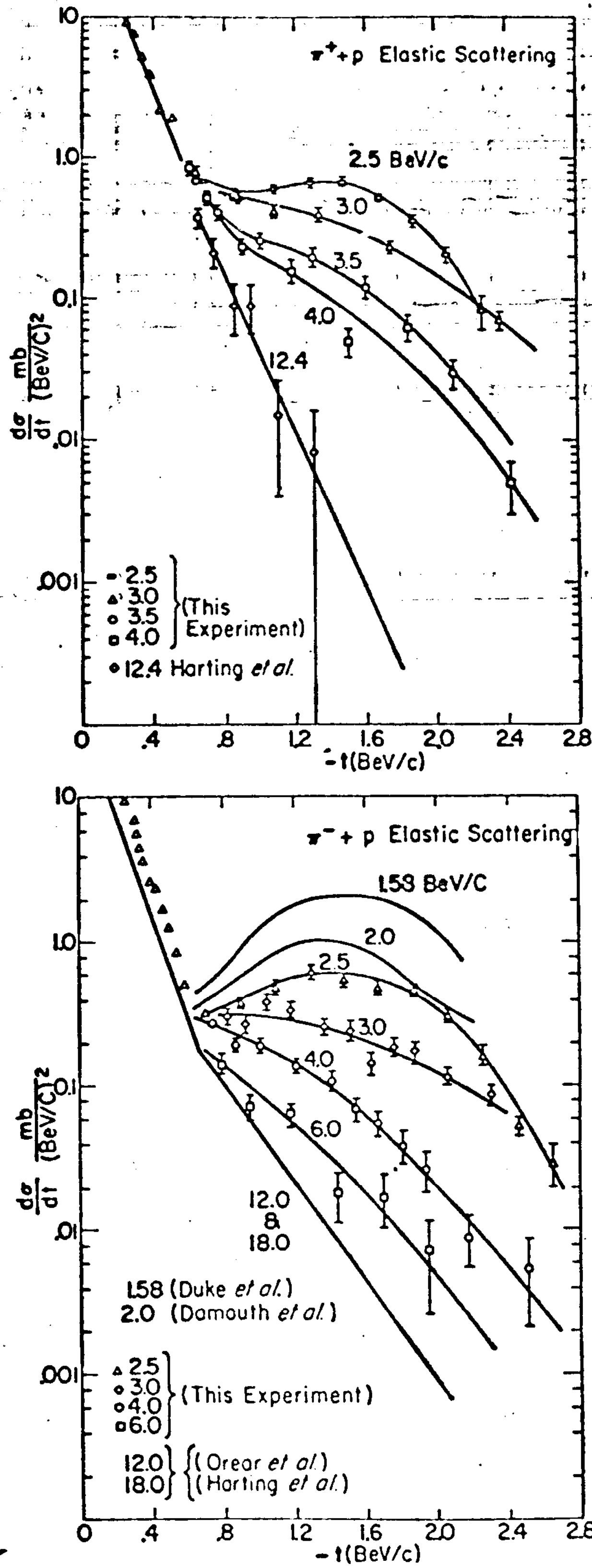

Fig. 15 Momentum dependence of the secondary peak in $\pi^+ + p$ and $\pi^- + p$ scattering. The low- and high-energy data are from Refs. 6, 7, and 8.

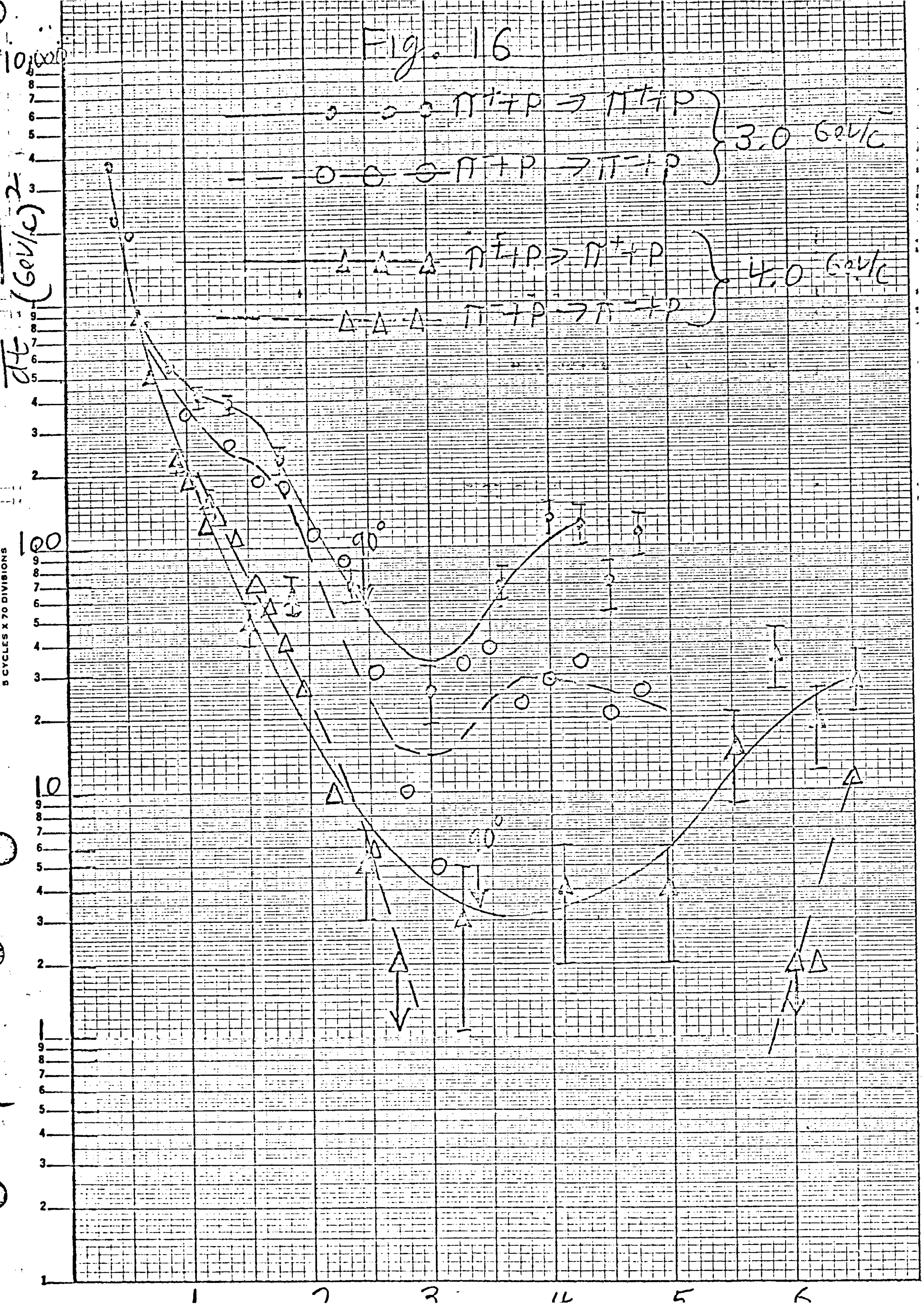

Fig. 16
π⁺+P → π⁺+P
π⁻+P → π⁻+P
3.0 GeV/c
π⁺+P → π⁺+P
π⁻+P → π⁻+P
4.0 GeV/c
dσ/dt μb/(GeV/c)²
90°
90°
10,000
100
10
1
1
2
3
4
5
6
K&E SEMI-LOGARITHMIC 358-91
KEUFFEL & ESSER CO. MADE IN U.S.A.
5 CYCLES X 70 DIVISIONS

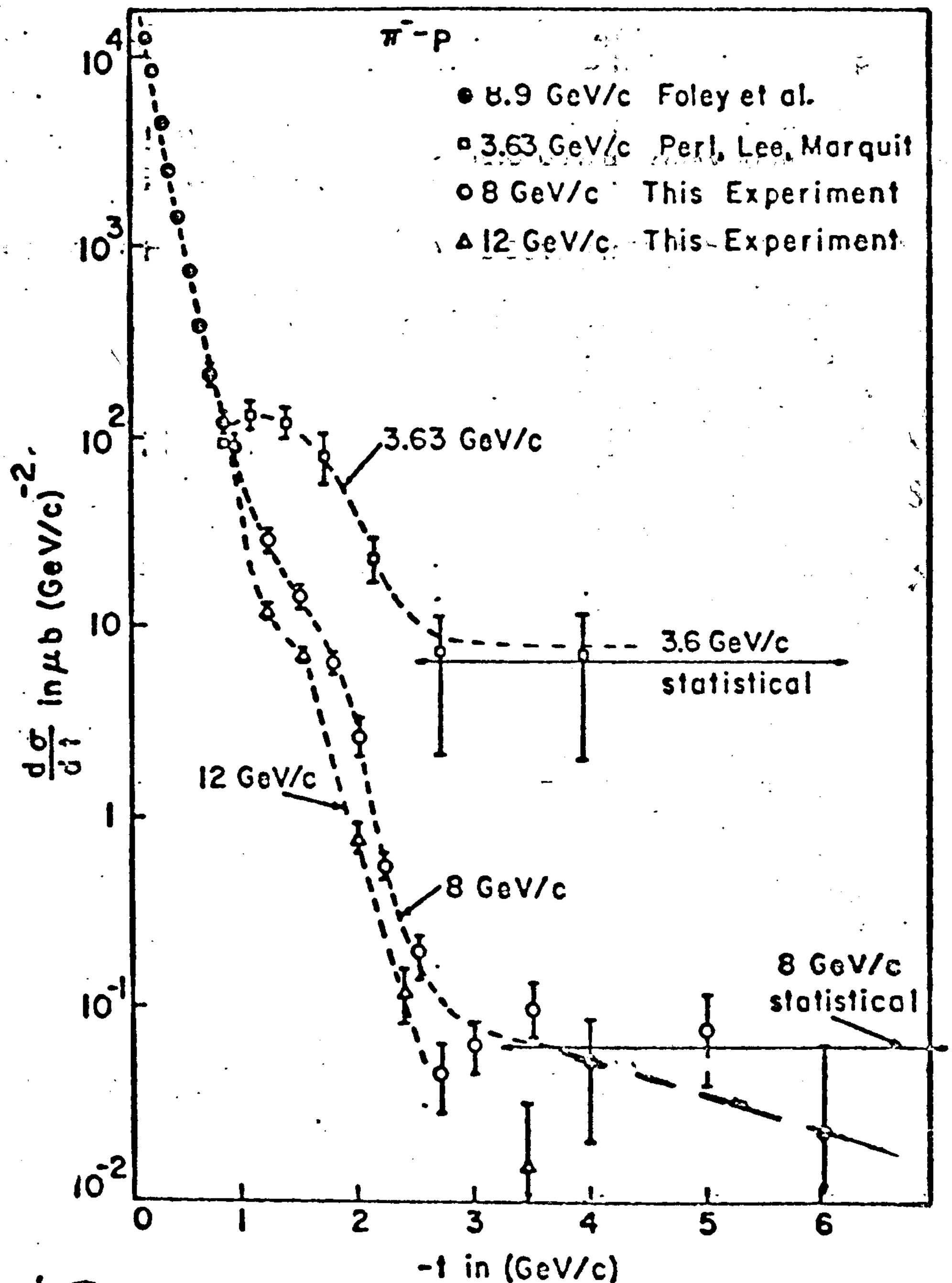

Fig. 17 Angular distributions for π^--p elastic scattering at lab momenta of 3.63, 8, and 12 GeV/c. Curves are drawn only as a guide.

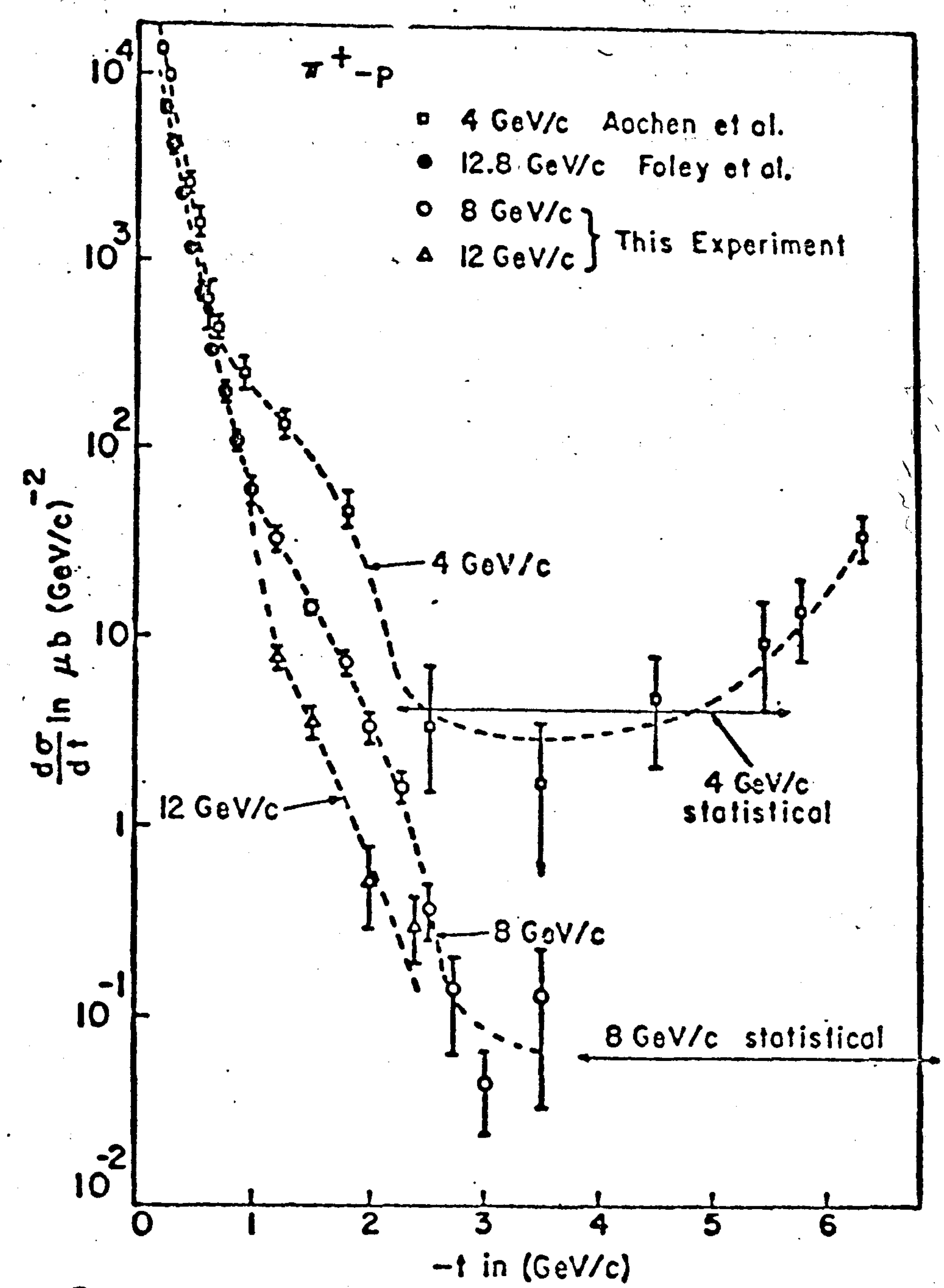

Fig 18 Angular distributions for π^+-p elastic scattering at lab momenta of 4, 8, and 12 GeV/c. Curves are drawn only as a guide.

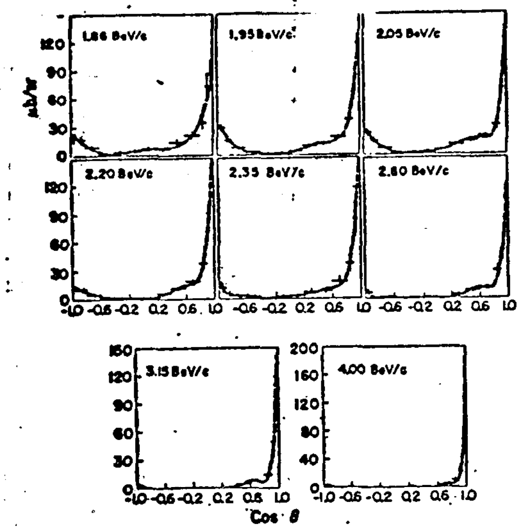

$\pi^- + p \Rightarrow \Lambda^0 + K^0$

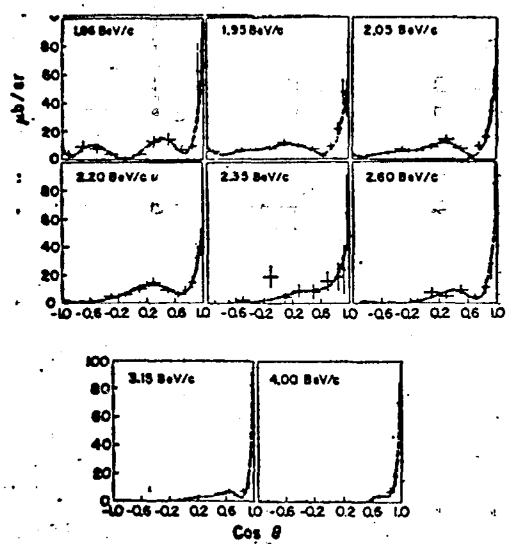

$\pi^- + p \Rightarrow \Sigma^0 + K^0$

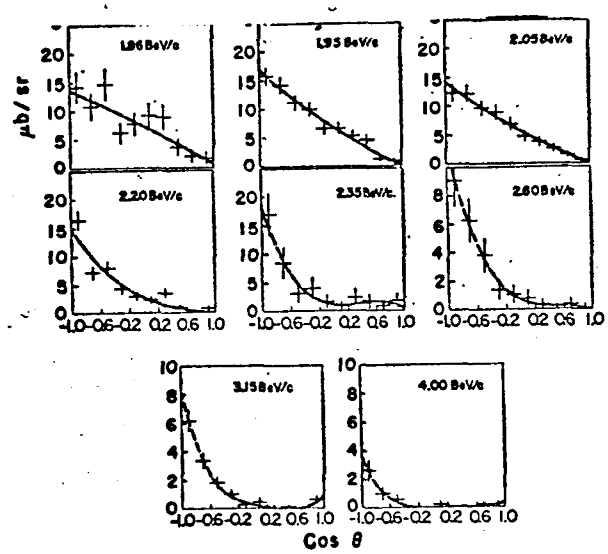

$\pi^- + p \Rightarrow \Sigma^- + K^+$

Fig. 19

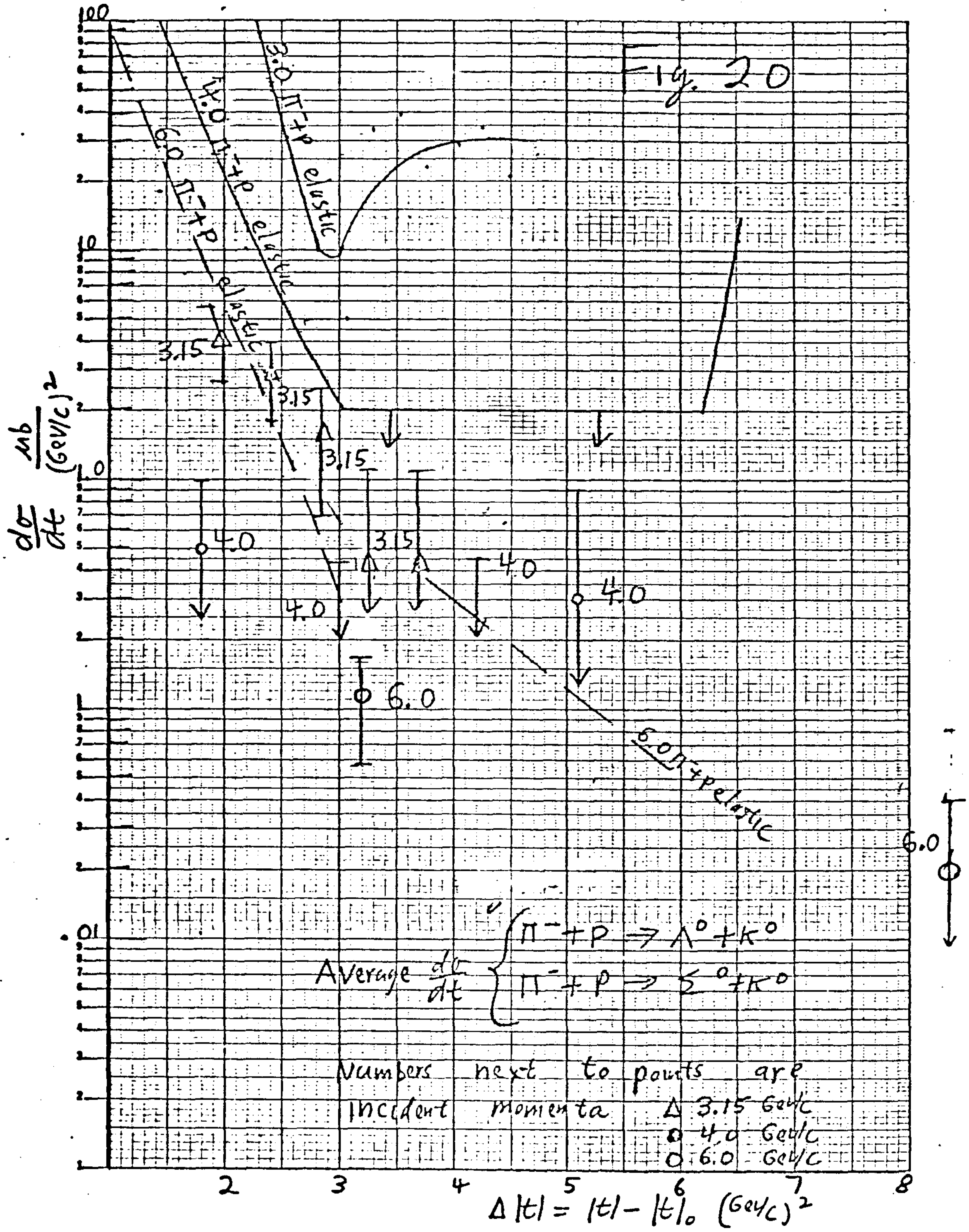

Fig. 20
3.0 π⁻+p elastic
4.0 π⁻+p elastic
6.0 π⁻+p elastic
6.0 π⁻+p elastic
3.15
4.0
6.0
Average dσ/dt { π⁻ + p → Λ° + K° ; π⁻ + p → Σ° + K° }
Numbers next to points are incident momenta
Δ 3.15 GeV/c
o 4.0 GeV/c
o 6.0 GeV/c
dσ/dt μb/(GeV/c)²
Δ|t| = |t| − |t|₀ (GeV/c)²
100
10
1.0
.01
2
3
4
5
6
7
8

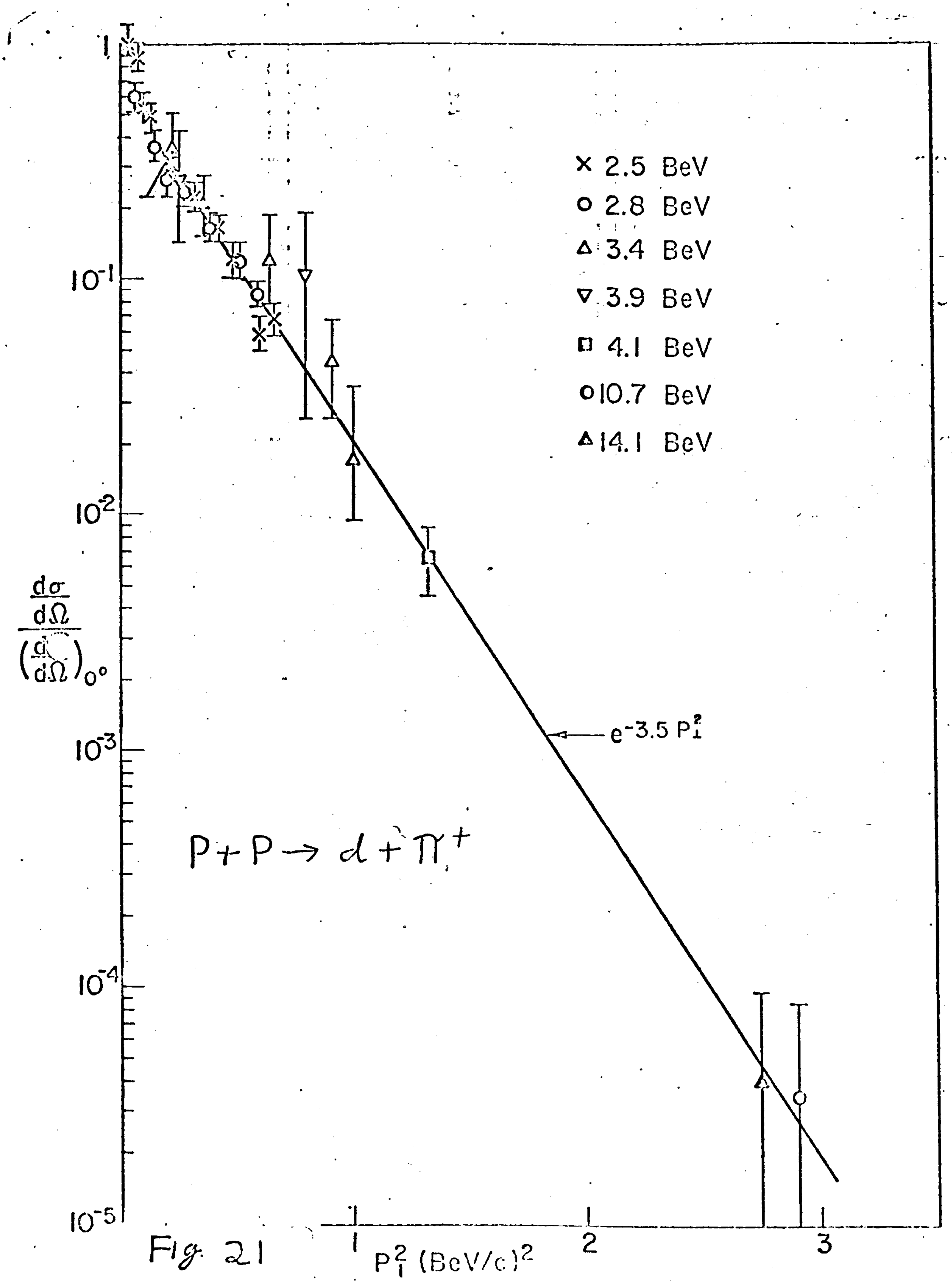

× 2.5 BeV
o 2.8 BeV
Δ 3.4 BeV
∇ 3.9 BeV
□ 4.1 BeV
o 10.7 BeV
Δ 14.1 BeV
$e^{-3.5 P_\perp^2}$
$P + P \to d + \pi^+$
$\frac{d\sigma}{d\Omega} / \left(\frac{d\sigma}{d\Omega}\right)_{0°}$
1
10^{-1}
10^{-2}
10^{-3}
10^{-4}
10^{-5}
1
2
3
$P_\perp^2$ (BeV/c)^2

Fig. 21

Fig 22

a) $\pi^+ p \Rightarrow \pi^+ p$

b) $\pi^+ p \Rightarrow \rho^+ p$

c) $\pi^+ p \Rightarrow \pi^0 N^{*++}$

d) $\pi^+ p \Rightarrow \rho^0 N^{*++}$

e) $\pi^+ p \Rightarrow \omega^0 N^{*++}$

f) $\pi^+ p \rightarrow A_2^+ p$

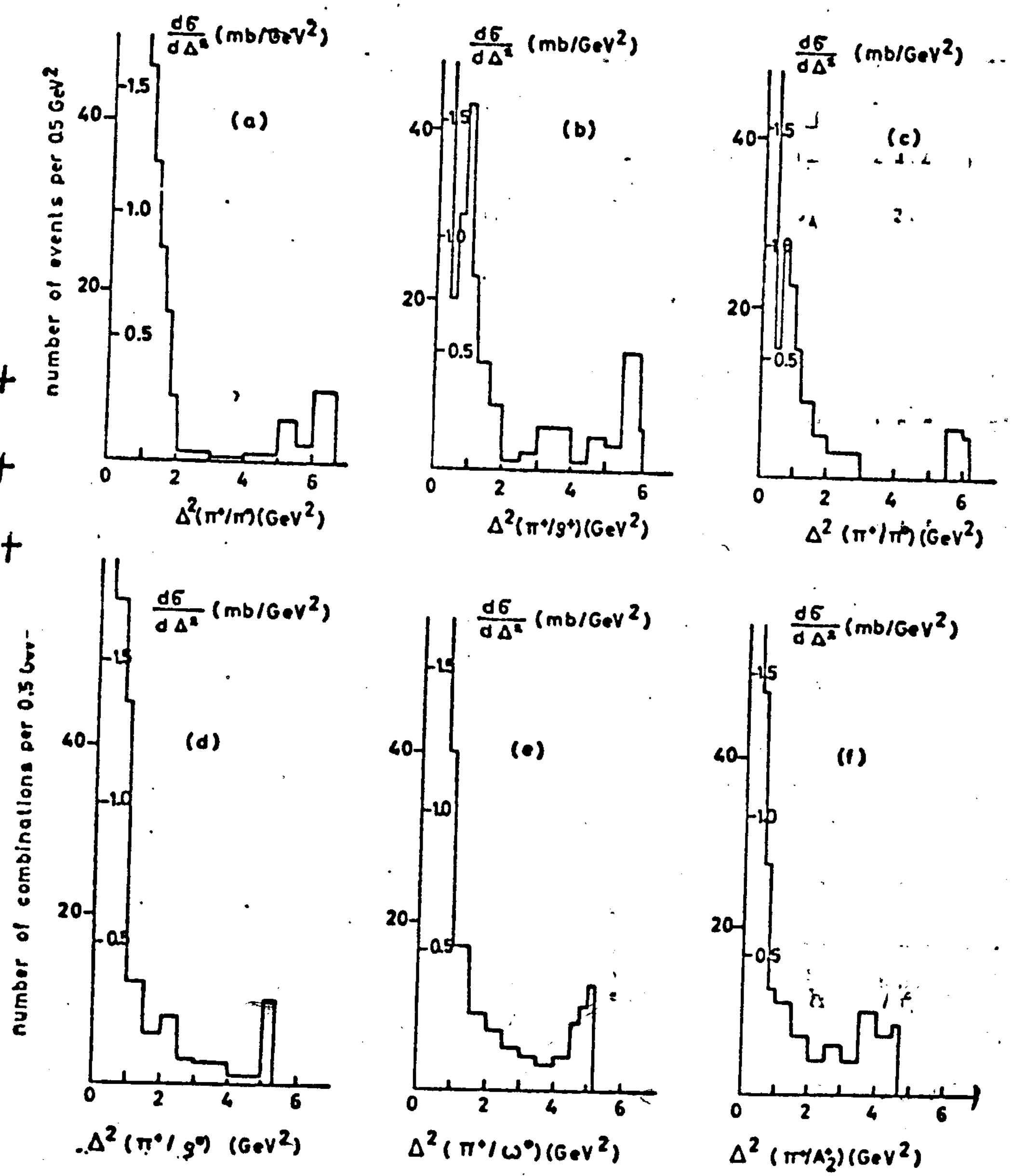

Fig. 23

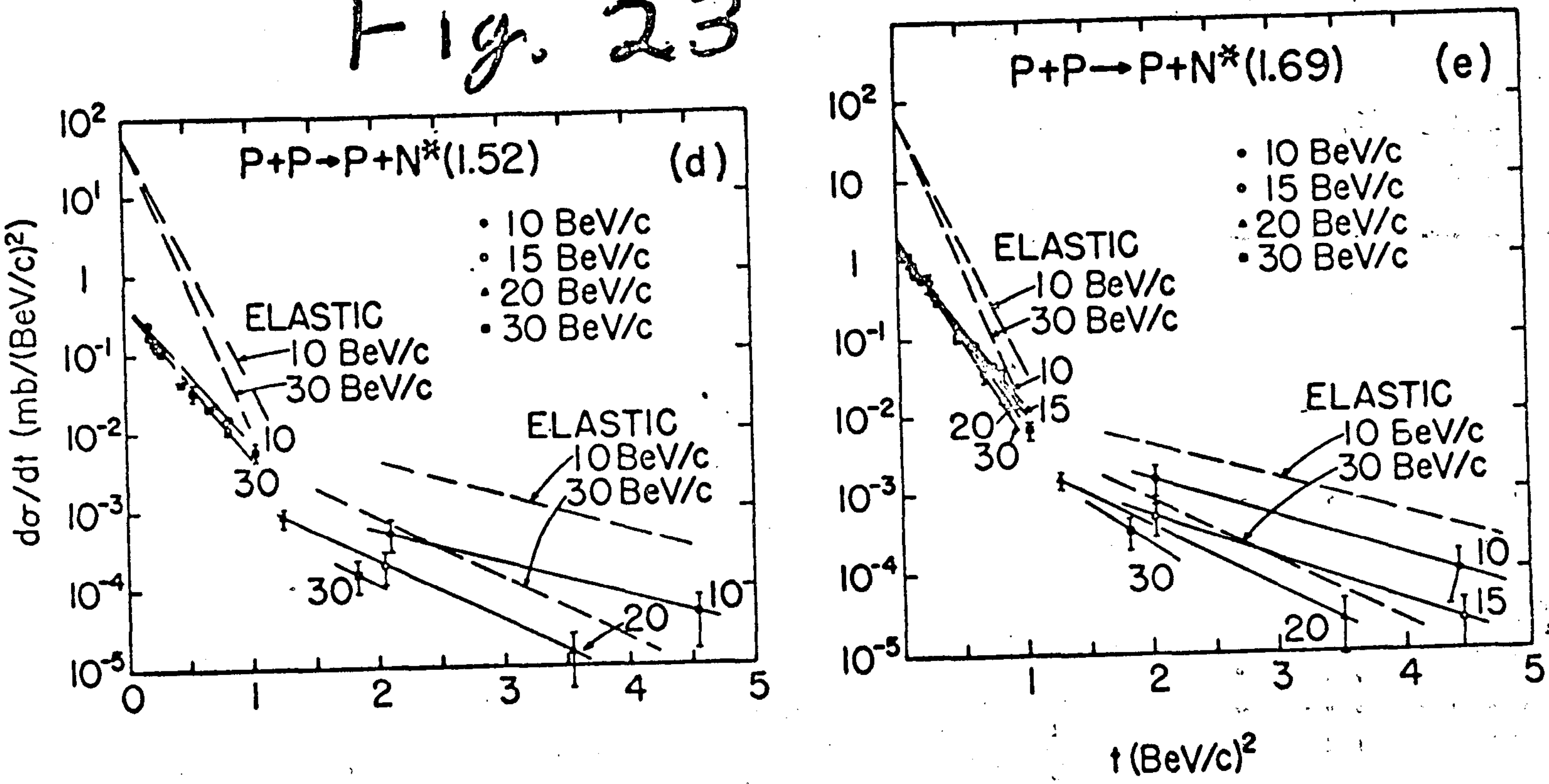
P+P→P+N*(1.52)
(d)
• 10 BeV/c
◦ 15 BeV/c
▴ 20 BeV/c
▪ 30 BeV/c
ELASTIC
10 BeV/c
30 BeV/c
10
30
ELASTIC
10 BeV/c
30 BeV/c
30
20
10
dσ/dt (mb/(BeV/c)²)
10²
10¹
1
10⁻¹
10⁻²
10⁻³
10⁻⁴
10⁻⁵
0
1
2
3
4
5
P+P→P+N*(1.69)
(e)
• 10 BeV/c
◦ 15 BeV/c
▴ 20 BeV/c
▪ 30 BeV/c
ELASTIC
10 BeV/c
30 BeV/c
10
15
20
30
ELASTIC
10 BeV/c
30 BeV/c
10
15
20
30
10²
10
1
10⁻¹
10⁻²
10⁻³
10⁻⁴
10⁻⁵
1
2
3
4
5
t (BeV/c)²